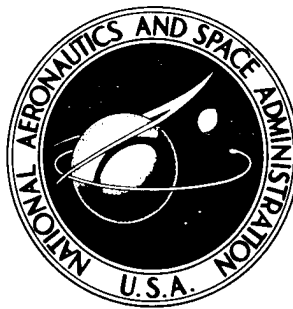


NASA TECHNICAL NOTE



NASA TN D-2864

NASA TN D-2864

# OPERATIONAL EXPERIENCE WITH THE X-15 REACTION CONTROL AND REACTION AUGMENTATION SYSTEMS

*by Calvin R. Jarvis and Wilton P. Lock*

*Flight Research Center*

*Edwards, Calif.*

OPERATIONAL EXPERIENCE WITH THE X-15 REACTION CONTROL  
AND REACTION AUGMENTATION SYSTEMS

By Calvin R. Jarvis and Wilton P. Lock

Flight Research Center  
Edwards, Calif.

NATIONAL AERONAUTICS AND SPACE ADMINISTRATION

---

For sale by the Clearinghouse for Federal Scientific and Technical Information  
Springfield, Virginia 22151 – Price \$2.00

OPERATIONAL EXPERIENCE WITH THE X-15 REACTION CONTROL  
AND REACTION AUGMENTATION SYSTEMS\*

By Calvin R. Jarvis and Wilton P. Lock

SUMMARY

The performance and operational characteristics of the two reaction control systems used in the X-15 airplane are discussed. Control of the X-15 during flight at low dynamic pressures was satisfactory with the manual acceleration command reaction controls. During the early stages of reentry, however, the control task was complicated by aerodynamic forces. The addition of a reaction augmentation system made the task easier. Although proportional controls were designed into the X-15 reaction control system, the pilot used them generally as on-off controls.

The problems encountered during the development of the reaction control system were the result of an unsuitable application of aluminum components in the hydrogen-peroxide system.

Aircraft structural vibration necessitated the addition of an electronic filter to the electronics assembly of the reaction augmentation system.

INTRODUCTION

The flight envelope of the X-15 airplane includes low-dynamic-pressure regions at high altitude in which the effectiveness of the aerodynamic controls is not sufficient to provide even marginally satisfactory control of the vehicle. As a result, a reaction control system was provided for controlling vehicle attitude in these regions.

Two different reaction control systems are used in the three X-15 research vehicles. (The airplanes are hereafter referred to as the X-15-1, X-15-2, and X-15-3.) The reaction control system discussed in this paper is used in the X-15-1 and X-15-2 vehicles and consists of both a manual and an automatic mode. An acceleration command mode, manually operated by the pilot, is used to control vehicle attitude. A rate-sensing reaction augmentation mode, added to both aircraft after installation of the acceleration command mode, provides

---

\*Some of the information presented herein was previously included in the paper "Operational Experience with X-15 Reaction Controls" (ref. 1) at the SAE-ASME Air Transport and Space Meeting, New York, N. Y., Apr. 27-30, 1964.

damping moments which stabilize the vehicle. The X-15-3 airplane utilizes a rate command, attitude-hold reaction control system (discussed in detail in refs. 1 and 2).

This paper describes the X-15 reaction control system and discusses the system characteristics, operational experiences, and development problems. Data are presented from X-15 high-altitude flights during which both the manual control and reaction augmentation systems were operated.

#### SYMBOLS

$a_n$	normal acceleration, g units
$d$	dead band, deg/sec
$e^{-st}$	time-delay function
$F_r$	rocket thrust, lb
$F_s$	stick force, lb
$f$	frequency, cps
$g$	acceleration due to gravity, ft/sec <sup>2</sup>
$h$	altitude, ft
$I$	vehicle inertia, slug-ft <sup>2</sup>
$I_{sp}$	specific impulse, sec
$I_t$	total impulse, lb-sec
$P_c$	chamber pressure, psia
$P_e$	nozzle exit pressure, psia
$p$	rolling angular velocity, deg/sec
$q$	pitching angular velocity, deg/sec
$\bar{q}$	dynamic pressure, lb/sq ft
$r$	yawing angular velocity, deg/sec

$s$	Laplace variable
$t$	time, sec
$t_{\bar{q} < 25}$	time below $\bar{q} = 25$ lb/sq ft, sec
$W$	propellant weight, lb
$\dot{W}$	propellant flow rate, lb/sec
$\alpha$	angle of attack, deg
$\beta$	angle of sideslip, deg
$\delta_a$	aileron deflection, deg
$\delta_h$	horizontal-stabilizer deflection, deg
$\delta_s$	stick deflection, percent of maximum
$\delta_v$	vertical-stabilizer deflection, deg
$\Phi$	phase angle, deg
$\varphi$	angle of bank, deg
$\omega_n$	natural frequency, radians/sec

## AIRPLANE

The X-15 (fig. 1) is a single-place, rocket-powered airplane designed for high-speed and high-altitude flight research. The airplane has been flown to speeds in excess of a Mach number of 6 and altitudes in excess of 350,000 feet. Because of this altitude capability, reaction jets as well as aerodynamic surfaces are used to provide adequate control and damping throughout the flight envelope. A lower ventral tail is also used to improve directional stability in some flight regions.

The pilot's controls (fig. 2) include a conventional center stick and rudder pedals, an aerodynamic controller (side stick) that is located on the right console and is interconnected with the center stick, and a three-axis controller (stick) on the left console for the jet reaction controls.

## DESCRIPTION AND OPERATION OF THE REACTION CONTROL SYSTEM

The X-15 reaction control system (RCS) is a hydrogen-peroxide monopropellant jet (or rocket) system which produces control torques about all three body axes. The system consists of a manual mode, operated by the pilot, and an automatic mode, which provides stability augmentation.

### Manual Reaction Control System

The X-15 manual reaction control system consists of two independent, parallel propellant and rocket systems that are usually operated simultaneously by a single three-axis control stick. Components of the two systems are shown schematically in figure 3.

The hydrogen-peroxide ( $H_2O_2$ ) propellant for the reaction control rockets is metered by pilot-controlled proportional valves. These valves are spool and sleeve arrangements which meter the hydrogen peroxide proportional to control-stick position. The metering valves for both systems are constructed so that separation of the two parallel systems is maintained at all times.

Each system uses six monopropellant reaction control rockets to develop the required accelerations about the three control axes. The locations of the control rockets in the X-15 are shown in figure 4. Two different types of rockets, designated as A and B (fig. 5), are used in each system. The A rockets are in the nose of the aircraft to provide the desired pitching and yawing moments; the B rockets are in the wings to give the desired rolling moment. Because of the limited area available inside the wings, the B rocket exhaust nozzle is positioned at right angles to the decomposition-chamber centerline. Design and performance parameters for the rockets are listed in table I.

Each rocket contains a silver-screen catalyst bed, with six separate cup assemblies in the A rocket and seven separate assemblies in the B rocket. Each assembly is composed of 15 silver screens and 1 corrosion-resistant screen. The catalyst decomposes the 90-percent  $H_2O_2$  propellant into a mixture of superheated steam and oxygen. The steam is then exhausted through a convergent-divergent nozzle to produce the desired control moment.

In normal operation, both manual reaction control systems function simultaneously. Each system was designed for a maximum angular acceleration of  $2.5 \text{ deg/sec}^2$  about the pitch and yaw axes and  $5 \text{ deg/sec}^2$  about the roll axes. When both systems are operating, each need function at only 50 percent of its maximum thrust level to obtain the airplane's maximum design angular acceleration. Should one system fail at any time during a flight, the remaining system may be operated at maximum thrust levels to obtain the maximum design acceleration.

The reaction control system controller is connected directly to the metering valves through a series of cables, rods, and bellcranks. Artificial feel is obtained by the use of spring-loaded bungees which provide fixed force

gradients and positive centering of the stick at all times. A schematic drawing of the mechanical linkage arrangement is shown in figure 6. The pilot operates the controller with his left hand, moving it up and down for pitch, left and right for yaw, and rotating it clockwise and counterclockwise for roll. In flight, the aircraft nose is propelled in the direction the controller is moved, and rolled in the direction of controller rotation.

### Reaction Augmentation System

Previous studies (refs. 3 and 4) indicated that, although satisfactory attitude control of a vehicle could be maintained with acceleration command reaction controls, the pilot had to give considerable attention to the control task. In order to decrease the X-15 piloting task in the low-dynamic-pressure flight regions, an automatic reaction augmentation system (RAS) was incorporated into the basic reaction control systems in the X-15-1 and X-15-2 airplanes. The RAS was added to only one of the two parallel reaction control systems on each aircraft, which, in effect, limits the RAS control authority to one-half that available to the pilot, who has command over both systems.

A block diagram of the RAS components is presented in figure 7. The RAS assembly consists, basically, of three rate gyros, which are located to sense the aircraft's rotational rates about all three body axes. The gyros convert the vehicle's angular rates to proportional electrical signals which are amplified in the electronics section of the assembly. The signal is then used to operate an on-off solenoid control valve which controls the flow of propellant to the rocket motors.

Switches on the controller linkages prevent opposing inputs from occurring between the RAS and the pilot. When the controller is displaced, the switch is in the open position and the RAS circuit is inoperative in the affected axis. When the controller is in the neutral position (no pilot input), the override switch is closed and the RAS automatically damps any rotational rate sensed by the gyros.

Threshold levels, in which the RAS will be inoperative, are pre-set during the ground checkout prior to flight. These thresholds are variable from 0.2 deg/sec to 2 deg/sec in pitch and yaw and from 0.5 deg/sec to 5 deg/sec in roll.

Individual, pilot-operated switches for engaging or disengaging the pitch, roll, or yaw channels of the system are also used. This arrangement enables the pilot to select any desired damper configuration. Cockpit indicator lights tell the pilot which channels are engaged.

An accelerometer unit (fig. 7) is used to provide a signal that will automatically disengage the system during reentry after normal aerodynamic effectiveness has been reestablished. This feature aids the pilot in disengaging the system and prevents excessive fuel usage. The pre-set normal-acceleration level at which this transfer occurs is variable from 1g to 3g. A manual override switch is also incorporated into the circuit, should the pilot choose to eliminate this feature.

## Propellant Supply System

A schematic diagram of one of the dual, identical X-15 reaction-control propellant supply systems is presented in figure 8. As shown, the  $H_2O_2$  is stored in a Vicone or Teflon bladder within an ellipsoidal pressure tank. Other components include a reaction control propellant shutoff and jettison valve operated by the pilot, a hydrogen-peroxide relief valve to prevent overpressurization, and a blowout plug which ruptures should the pressure-relief valve malfunction and overpressurization occur.

Each of the  $H_2O_2$  supply systems also supplies propellant to separate auxiliary power turbines which provide electrical and hydraulic power for the aircraft. Thus, the  $H_2O_2$  tanks must be large enough to store enough propellant for each auxiliary power unit and the reaction control rockets. The maximum capacity of each tank is 155 pounds of  $H_2O_2$ . The unusable propellant in each system is about 12 pounds. Since each auxiliary power unit requires approximately 85 pounds of  $H_2O_2$  during an X-15 flight, 58 pounds are available in each system for use as reaction control propellant. Should more  $H_2O_2$  be required, however, the pilot may transfer it from a rear storage tank which supplies propellant to the turbine pumps of the main rocket engine.

When pressurized helium is injected between the expulsion bladder and the wall of the hydrogen-peroxide storage tank (fig. 8), pressure is exerted on the collapsible bladder, which forces the peroxide out of the tank through a metal standpipe and propellant pickup tube. With this arrangement, positive propellant flow is obtained regardless of the aircraft's attitude. In addition, any "fuel-floating" problems that might occur during the zero-gravity portion of a flight are eliminated.

After 80 percent of the hydrogen-peroxide propellant is expelled, the expulsion bladder collapses down to the standpipe. Pressure is exerted on the standpipe but not on the remaining peroxide, and, therefore, a pressure differential exists between the  $H_2O_2$  inside the standpipe and the helium outside the standpipe. When this pressure differential reaches 30 psi to 40 psi, a pressure-differential switch is actuated to close a circuit to an " $H_2O_2$  low light" in the pilot's cockpit. When the pressure differential reaches 55 psi, a valve opens to admit helium on top of the remaining peroxide inside the standpipe, forcing the  $H_2O_2$  through the propellant pickup tube. After the expulsion bladder has collapsed around the standpipe, the system is no longer a positive-flow type but becomes a standard pressure-feed system, which requires that the pilot keep the aircraft in a normal attitude at a positive normal acceleration in order to obtain continuous flow. This requirement does not pose any problem; by the time 80 percent of the propellant has been consumed, the aircraft should be well within the region where the aerodynamic control effectiveness will be adequate. Moreover, if necessary, the pilot can transfer hydrogen peroxide from the X-15 rocket-engine propellant-pump supply tanks, as previously discussed.



## DISCUSSION

### System Characteristics

Three-axis controller.— Figures 9(a) to 9(c) show the relationship between RCS controller displacement and the applied force for the pitch, roll, and yaw axes, respectively, and, also, compare design characteristics with X-15 ground-test data. As noted previously, spring-loaded bungees are installed in the mechanical linkage of the system to oppose movement of the controller in all directions. Double bungees are used in the pitch and yaw linkages (figs. 9(a) and 9(c)) and provide a noticeable increase in the force with which they oppose movement of the controller at the half-thrust point of operation.

Figures 10(a), 10(b), and 10(c) show the relationship between RCS rocket thrust, as determined from ground-calibrated chamber-pressure transducers, and controller position for the pitch, roll, and yaw, axes, respectively. In addition, design values are compared with X-15 flight data. Also shown is the  $\pm 15$ -percent stick-deflection dead band that was built into the system to reduce the possibility of inadvertent pilot inputs.

Attitude rockets.— The variation of propellant flow rate and chamber pressure with rocket-motor thrust is presented in figure 11(a) for the pitch and yaw (type A) control rockets and in figure 11(b) for the roll (type B) control rockets. These data were obtained from ground tests conducted at an altitude of 2,200 feet and under atmospheric pressure conditions. The roll rockets were designed for a maximum thrust of 40 pounds and the pitch and yaw rockets for a maximum thrust of 113 pounds, at an altitude of 200,000 feet.

Control authority.— The maximum angular accelerations to be provided originally by each of the X-15 reaction control systems were as follows:

Mode	Angular acceleration, deg/sec <sup>2</sup>
Pitch	2.5
Roll	5.0
Yaw	2.5

Calculations based on the original X-15 design inertias and control-rocket moment arms (fig. 12) showed that rocket thrusts of 113 pounds in pitch and yaw and 40 pounds in roll (for a design altitude of 200,000 ft) would more than satisfy the maximum acceleration requirements. However, because of the continuing increase in airplane weight and the attendant changes in moments of inertia during the design period, it was discovered that the thrust levels of the pitch and yaw rockets were too low to meet the previously established acceleration requirements. The moments of inertia and angular accelerations of the present vehicle are as follows:

Axis	Actual inertia, slug-ft <sup>2</sup>	F <sub>r</sub> , lb	Maximum angular accel- eration, deg/sec <sup>2</sup>
Pitch	84,800	113	2.01
Roll	3,600	40	5.85
Yaw	86,500	113	1.97

The roll acceleration meets the original design requirement; however, the maximum pitch and yaw accelerations are significantly lower than the original values. Since both rockets in each axis of the dualized system function during normal operation of the X-15 reaction controls, the combined rocket thrusts easily meet the airplane requirements.

Fuel requirements.— The specific impulse associated with each attitude rocket (determined from experimental data obtained by the rocket manufacturer) and the estimated total impulse and fuel consumption about each axis (using the original X-15 design inertias) for each reaction control system are as follows:

Axis	I <sub>sp</sub> , sec	I <sub>t</sub> , lb-sec	W, lb
Pitch	158	1302	8.2
Roll	139	626	4.5
Yaw	158	1716	10.9

During normal operation of the X-15 aircraft, the reaction control system is checked out before launch. In this checkout, each RCS rocket is fired for approximately 3 seconds to insure satisfactory operation. The estimated average amount of fuel used by each system during the checkout phase is as follows:

Mode	W, lb
Pitch	4.6
Roll	1.7
Yaw	4.6

The total estimated fuel requirement for each system is, then, 34.5 pounds.

Analog-simulator studies (ref. 5), conducted to investigate the fuel requirements of the X-15 reaction augmentation system for typical altitude missions, indicated that the requirements depended primarily on the threshold settings and the control authority. For threshold settings of  $\pm 0.5$  deg/sec,  $\pm 1.0$  deg/sec, and  $\pm 0.5$  deg/sec and assumed maximum control-effectiveness values of  $2.2$  deg/sec<sup>2</sup>,  $5.8$  deg/sec<sup>2</sup>, and  $2.2$  deg/sec<sup>2</sup> in pitch, roll, and yaw, respectively, a maximum total impulse requirement of 4,800 lb-sec was obtained. These values resulted in a total estimated fuel requirement of 32 pounds. It was anticipated that this requirement would be well within the 155 pounds of propellant available for the auxiliary power unit and the reaction control system.

## Flight Experience

The acceleration command and augmentation reaction control systems have been operated on 18 X-15 flights. Twelve of the flights were made using only the acceleration command system; both systems were used on six flights. On 12 of the 18 flights, the systems were operated at moderate-dynamic-pressure conditions, during which there was sufficient aerodynamic control authority to maintain aircraft stability and control. Tests were made at these conditions to check out the systems and to familiarize the pilot with system response. During six flights the dynamic pressure decreased to less than 25 lb/sq ft, which necessitated RCS operation to stabilize the aircraft. On three of these flights, control of the vehicle was accomplished by using only the manual acceleration command system in the low-dynamic-pressure environment.

A typical X-15 high-altitude flight profile is shown in figure 13. Following launch and engine ignition, a constant-acceleration pullup is initiated and held until the desired pitch attitude is reached. The pilot then usually flies a constant pitch angle with aerodynamic controls until engine burnout occurs and low dynamic pressures are encountered. He then makes a transition from aerodynamic to reaction controls. In this low-dynamic-pressure region, the pilot makes compensatory control inputs to maintain the desired aircraft attitude. After the peak altitude is reached, the aircraft begins its descent, and it is necessary to establish and maintain a reentry angle of attack. As the dynamic pressure and normal acceleration increase at reentry, the pilot performs a 3g to 5g pullout maneuver until the recovery is completed. The reaction control system is sufficiently effective to be useful for damping small perturbations down to an altitude of approximately 100,000 feet or a dynamic pressure of 200 lb/sq ft. The changeover from manual reaction controls to aerodynamic controls is made at the pilot's discretion, inasmuch as aerodynamic control effectiveness is recovered during the reentry maneuver. During this transition, the pilots sometimes operate the aerodynamic and the reaction control systems simultaneously. Experience has also shown that pilots tend to use the reaction controls, during reentry, to higher dynamic pressures than originally anticipated in the system design.

Manual reaction control system.— Figure 14 is a time history of several parameters recorded during the portions of a high-altitude X-15 flight in which the dynamic pressure was extremely low. The reaction augmentation system was not used during this flight, and the aircraft was flown with the lower ventral tail on. The maximum altitude attained was 247,000 feet. The transition from aerodynamic to reaction controls was made immediately after engine burnout ( $t \approx 85$  sec,  $h \approx 140,000$  ft). For approximately 147 seconds, the dynamic pressure was less than 25 lb/sq ft. During this time, the aircraft was essentially controlled by using the reaction control rockets. The reaction control inputs shown in the figure are indicative of the duty cycle, rather than the amplitude of rocket thrust or pilot input.

The pilot was able to maintain adequate control of the vehicle during the low-dynamic-pressure portion of the climbout and the early stages of reentry, even though damping moments had to be applied manually, which required considerable concentration on the control task. A three-axis ball was used for

attitude reference. Most of the pilot's inputs were compensatory or corrective. He did, however, perform a planned  $-20^\circ$  bank-angle maneuver using only the reaction controls.

A  $-25^\circ$  horizontal-stabilizer nose-up trim deflection was initiated at  $t \approx 220$  seconds, prior to reentry. During the reentry, it was found that the ability to maintain the desired angle of attack during the rapid dynamic-pressure buildup was degraded because of aerodynamic effects. This degradation is shown by the oscillations about all three axes from 240 seconds to 270 seconds. The amplitude of motions about the pitch, roll, and yaw axes built up during the early portion of this time interval, where aerodynamic damping was poor. The pilot was kept extremely busy trying to maintain the reentry angle of attack while, at the same time, manually damping out roll and yaw motions which resulted from the increasing dynamic pressure. It was also necessary for him to determine the point at which the reaction controls ceased to be effective in controlling the aircraft and to revert to the normal aerodynamic controls. When it is realized that these simultaneous functions were compressed into only a few seconds, the magnitude of the control task during this portion of the flight is evident. The pilot rated the overall reentry control task, below a normal acceleration of  $4g$ , at 2, 3, and 4 for pitch, roll, and yaw, respectively, based on the Cooper scale (ref. 6).

Data from the  $-20^\circ$  bank-angle maneuver (fig. 14) are shown on an expanded time scale in figure 15. Presented are RCS stick deflection, rocket thrust, and the resulting bank angle. The proportional-thrust characteristics of the acceleration command system were used to some extent during the maneuver, as shown by the difference in the amplitudes of the stick displacements and the resulting rocket thrusts. The short pulse-type control inputs characteristic of on-off acceleration command systems are, however, present. X-15 flight experience has shown, in fact, that pilots tend to use the system in an on-off manner rather than as a proportional-thrust system; thus, it appears that comparable control characteristics can be attained with a much simpler on-off thrust control system. A similar finding is discussed in reference 7, which indicates, also, that the nature of the control task has some effect on the similarity between control with on-off and proportional acceleration command systems.

Reaction augmentation system.— Figure 16 is a time history of the high-altitude portion of an X-15 flight during which the manual reaction control and reaction augmentation systems were both operated. The ventral tail was removed for the flight after it was found that the ventral-on configuration showed undesirable control characteristics in certain regions of the flight envelope (ref. 8). The pilot transferred from aerodynamic to manual reaction controls immediately after engine burnout and also engaged the reaction augmentation system. RAS threshold settings were  $0.5$  deg/sec in pitch and yaw and  $1$  deg/sec in roll. The control task was to maintain pitch and roll attitude to within  $\pm 8^\circ$  throughout the low-dynamic-pressure and early reentry portions of the flight. The lower-amplitude pulses shown in the figure were produced by the reaction augmentation system; the higher pulses are from manual inputs. The maximum altitude attained was 226,400 feet.

The portion of the flight in which the reaction augmentation system was used lasted approximately 3 minutes, after which the system was automatically disengaged by the accelerometer cutoff switch. Relatively few manual inputs were required to establish the desired attitude in the low-dynamic-pressure region, as compared to the flight shown in figure 14 in which only the manual system was used. Although the fewer inputs could have resulted from the  $-20^\circ$  bank-angle maneuver performed with the manual system, the increased damping provided by the reaction augmentation system is believed to be a significant factor. The scheduled  $18^\circ$  reentry angle of attack for this flight was held to within  $2^\circ$ . The roll and yaw oscillations experienced during reentry with the manual system in the flight shown in figure 14 were considerably reduced in this flight when the RAS was used. The improvement in the pilot's ability to accomplish the reentry control task is reflected in the improved pilot ratings. The initial phase of the reentry was rated as 2, 1, and 1.25 for pitch, roll, and yaw, respectively.

Although the increased damping provided by the RAS during the initial reentry phase would account for the improved rating of the control task during this period, some of the improvement is also attributed to the removal of the ventral. The effect of the additional damping provided by the RAS, with the ventral, is shown in figures 17 and 18, analog time histories of reentries made with the six-degree-of-freedom X-15 flight control simulator. Figure 17 shows data from a reentry from an altitude of 300,000 feet without RAS damping and with the ventral on. The results are similar to those experienced during the actual flight made under the same conditions (fig. 14). Figure 18 is a simulator time history of a 300,000-foot reentry made with RAS damping and with the ventral on. Comparison of this figure with figure 17 shows that much of the reduction in vehicle motions can be attributed to the damping provided by the RAS, even with the airplane in the ventral-on configuration.

The considerable improvement in the reentry control task for the flight shown in figure 16 (ventral off, RAS on) over the reentry task for the flight shown in figure 14 (ventral on, RAS off) provides an example of the two techniques generally employed in solving problems of this nature: improving the stability of the vehicle by design modification and/or by artificially increasing damping through use of independent subsystems.

Fuel consumption.— The total amount of propellant used by the RCS, the corresponding time below a dynamic pressure of 25 lb/sq ft, and the average rate of fuel consumption during this period for four high-altitude flights of the X-15 are shown in the following table:

Flight	System	W, lb	$t_{\bar{q}} < 25$ , sec	Average rate of fuel consumption, lb/sec
A	Manual	84	115	0.730
B	Manual	28	73	.384
C	Manual	63	148	.425
D	Manual and RAS	72	128	.562

During flights A, B, and C, only the manual acceleration command system was used to stabilize and maintain control of the vehicle in the low-dynamic-pressure region. Both the RAS and manual systems were operated during flight D. The same pilot flew flights B, C, and D; a different pilot flew flight A. The primary task was to maintain the desired attitude angles of the vehicle in the low-dynamic-pressure regions and early stages of reentry. A  $-20^\circ$  bank-angle maneuver was performed during flight B.

The large average rate of fuel consumption on flight A resulted from the pilot's inadvertent trimming of the aerodynamic controls to a  $0^\circ$  angle of attack while he attempted to maintain an angle of attack of  $10^\circ$  with the RCS during reentry. Overcoming the aerodynamics of the airplane during reentry with RCS control inputs resulted in the large consumption of propellant.

The average rate of fuel consumption in flights B and C was approximately the same, with a slightly lower rate for flight B, even though a roll task was performed. A significantly larger amount of propellant was consumed during flight D, however, as a result of the RAS operation, which provides tighter attitude control and, thus, many more control inputs and rocket pulses.

#### DEVELOPMENT PROBLEMS

Many of the development problems experienced with the X-15 reaction control system were similar to problems encountered previously with comparable systems on other vehicles (refs. 9 and 10).

##### Manual Reaction Control System

Most operational problems encountered during the development of the X-15 reaction control system were concerned with the hydrogen-peroxide propellant system. Specific problems involved the reliability of the expulsion system, valves, and catalyst beds, and the proper selection and fabrication of materials.

Hardware material.— Because of the corrosive nature of the 90-percent concentrated  $H_2O_2$ , difficulties were encountered in finding materials that were

compatible with the propellant and would not deteriorate. A suitable material for the expulsion bladder was especially difficult to find. A material was needed that would be compatible with the  $H_2O_2$  propellant under long-time exposures, could withstand repeated flexing without fatigue or rupture under high-load conditions, and would have low-temperature capabilities. Two types of bladders are now being used, one constructed of Teflon, the other of Vicone, a fluorosilicone rubber. Both types have functioned satisfactorily except for a tendency to rupture along the creases that are formed when full expulsion of the propellant has occurred and the bladder is compressed around the standpipe. This problem has resulted in an inconsistent bladder life.

The original X-15 reaction control system was constructed entirely of aluminum. It was discovered, however, that chemical reaction between the aluminum and the hydrogen-peroxide propellant caused the formation of hydroxides. Deposits of these chemically formed substances resulted in stuck valves, short catalyst-bed life, and other component failures. Certain components which came into direct contact with the peroxide propellant were then constructed of stainless steel to eliminate the chemical reaction. Use of the two different metals, however, resulted in electrolytic action whenever the metals were joined and came into contact with hydrogen peroxide. This action caused various component failures and contaminated the propellant system with hydroxides.

The original propellant metering valves were twin poppet and sleeve arrangements constructed partly of aluminum alloys. Because of corrosive problems which prevented satisfactory operation, the valves were redesigned for construction with stainless steel. The redesigned valves showed galling and sticking characteristics during qualitative testing programs, so other design modifications—primarily a change in tolerances—were made. These modifications solved the problem satisfactorily. Eventually, the entire system was constructed of stainless steel in order to eliminate the corrosion problem.

Another problem was the difficulty in obtaining a leak-tight fit between the rocket-motor injectors and the combustion chambers, which were originally bolted together. The large quantities of heat ( $1,300^\circ F$ ) generated in the combustion chambers, as a result of the decomposition process, caused a differential thermal expansion which resulted in  $H_2O_2$  leakage between the mating surfaces of the injector and the rocket-motor casing. The problem was solved temporarily by welding the injector to the motor casing. This modification eliminated the leakage problem but made periodic inspection of the catalyst-bed assemblies impossible and generated new problems when catalyst replacement became necessary. The rocket-motor casing was later redesigned, and a special all-metal seal was fabricated to provide a leak-tight fit between the injector and the motor casing. The seals have not proved to be entirely leak-free, however, so the welded units are still in use.

Heat.— The local heat generated by the rocket motor during the decomposition process also caused severe damage to the injector check valves which were originally located adjacent to the rocket-motor assemblies. The heat resulted in extensive valve-seat damage and loss of spring temper, which caused a continuous flow of peroxide through the control rockets. This problem was

alleviated by moving the injector check valves upstream approximately 20 inches to prevent the heat generated by the rocket motors from affecting their operation.

Pressure surges.— During early qualification tests of the system, it was also discovered that transient pressure surges, resulting from valve operations, were large enough to unseat or open emergency pressure-relief devices and blow-out plugs, causing loss of the propellant. The pressure-relief devices were subsequently modified to allow for the pressure surges caused by valve actuation. Slower-operating valves were also utilized in some instances to reduce pressure surges.

Environmental conditions.— Environmental temperature conditions also necessitated special design consideration in the early development of the RCS. Because of the proximity of the  $H_2O_2$  flow lines to the X-15 liquid-oxygen storage tank, the lines had to be heated to prevent the propellant from freezing. Wraparound-type heaters were used on all peroxide flow lines. The reaction control metering valves were also heated to maintain temperatures in the range of 59° F to 74° F necessary for normal operation. In addition, electric heaters were installed around the rocket-motor decomposition chambers (fig. 5) to reduce the frequency of "wet" starts.

Controller sensitivity.— Inadvertent control inputs resulting from the three-axis controller configuration were difficult to eliminate. Inadvertent coupling between roll and yaw was especially objectionable. Increased stick-force gradients and wider dead bands provided improved control harmony and fewer coupled inputs.

### Reaction Augmentation System

Structural resonance.— During the initial flight-test phase of the reaction augmentation system, 13 cps oscillations were observed in the control rocket chamber pressures. After further investigation, it was found that these chamber-pressure oscillations corresponded to structural vibrations of the horizontal stabilizers. Because of the reaction between the aircraft fuselage and the horizontal tail, the RAS gyros were sensing the vibration and causing the rockets to respond to the structural resonant frequency. A similar problem encountered with the X-15 aerodynamic stability augmentation system is discussed in reference 11.

The nature of the oscillation problem is illustrated in figure 19 by means of a block diagram of the X-15 reaction augmentation system. The dynamic-response characteristics of the aircraft are represented in the forward loop of the diagram. The RAS elements are located in the feedback loop. When the structural vibration occurs, the RAS gyro senses the angular velocity of the fuselage and reacts to the vibration in the same manner in which the aircraft rotational rate is sensed. The rocket motors are then forced to operate at the 13 cps structural-vibration frequency.



Since this problem was of an inertial nature, resulting from the coupling between the X-15 horizontal tail and fuselage structure, the overall dynamic stability of the vehicle was not appreciably affected. The vibration did result, however, in excessive propellant consumption and loss of reaction control damping.

A method for eliminating this vibration problem is presented in the appendix. The method consists, basically, of incorporating an electronic filter to sufficiently attenuate the RAS signal at the 13 cps frequency so that the solenoid valve will not operate. Analytical and analog-computer studies indicated that a second-order filter with a natural frequency of 3 cps and a damping ratio of 0.5 would be adequate.

#### CONCLUDING REMARKS

The X-15 program has provided an opportunity to assess the problems of controls and operational methods required for stabilizing manned aircraft in low-dynamic-pressure regions and in establishing reentry attitude for reentries from high altitudes.

Satisfactory control of the X-15 was maintained during the portions of high-altitude flights in which the dynamic pressure was extremely low by means of the manual acceleration command reaction control system. The system was effective in providing the necessary moments about each axis to enable the pilot to maneuver and maintain a desired vehicle attitude angle.

The increasing dynamic pressure during reentry, which caused aerodynamic coupling between roll and yaw, markedly complicated the control task with the manual acceleration command system.

The reaction augmentation system significantly reduced the control task involved in maintaining proper aircraft attitude in regions of low dynamic pressure and during the initial stages of reentry.

Proportional-control characteristics were not used to the extent anticipated in the original design.

Extensive modifications to the original hardware of the reaction control system were required before an operational system was attained. Many problems were encountered during the initial test phase of the system as a result of an unsuitable application of the original fabrication material in the hydrogen-peroxide system.

Structural vibrations, sensed by the reaction augmentation system rate gyros, resulted in undesired control rocket operation. An electronic filter appears to have alleviated the problem, although no flights with the modified unit have been made.

Flight Research Center,  
National Aeronautics and Space Administration,  
Edwards, Calif., March 5, 1965.

## APPENDIX

### ANALYSIS OF X-15 REACTION AUGMENTATION SYSTEM STRUCTURAL-VIBRATION PROBLEM

The frequency response of the X-15 reaction augmentation system was obtained experimentally in order to determine the response characteristics of the system. The test was conducted on the aircraft with the propellant supply system fully pressurized. The RAS gyro assembly was placed on an oscillatory rate table to provide constant-amplitude rate inputs at various frequencies (input amplitude = 10 deg/sec). The results of the test are shown in figure 20, which presents the open-loop amplitude and phase-response characteristics of the RAS with the production shaping incorporated. The amplitude ratio, in terms of rocket thrust divided by gyro rate input, is plotted in decibels. The circles represent data obtained from the frequency-response tests. The solid lines represent results of analytical studies which used the describing-function method of nonlinear-control-system analysis and the component characteristics shown in figure 21. Results of analog studies are shown by the dashed lines.

The results obtained from the various methods are in good agreement. Each method tends to show that the response is essentially flat out to about 5 cps, where it begins to drop off. At 13 cps the frequency response obtained with the actual hardware shows that the amplitude ratio has dropped only 4 decibels, which means that the control rockets are functioning at about 64 percent of maximum thrust. The phase crossover point also occurs at a frequency of about 13 cps.

Several methods of eliminating the response of the system to the structural vibration were investigated. The most promising proposal seemed to be to alter the shaping network to make the system insensitive to frequencies higher than about 10 cps; a method by which this can be accomplished is illustrated in figure 21. This figure shows the dynamic-response characteristics of the individual RAS components. The gyro used in the system is a conventional second-order device with a natural frequency of 22 cps and a damping ratio of 0.3. The output of the gyro is limited by a saturating amplifier to an equivalent of 5 deg/sec of rate input, which, in effect, limits the gyro to a 5 deg/sec output signal. The shaping shown is the original production shaping and consists, simply, of a first-order lag with a break frequency of 8 cps. This shaping serves to attenuate the overshoot characteristics of the underdamped gyro and also filters out the 400 cps carrier inherent in the gyro output signal. The solenoid control-valve characteristics are those of a relay incorporating a variable dead-band setting. The dead-band setting in this instance is variable from 0.5 deg/sec to 5 deg/sec of equivalent input rate. The dynamic characteristics associated with such components as the propellant flow lines and check valves are represented by a simple time-delay function  $e^{-st}$  ( $t = 0.055$  sec). The control-rocket characteristics were determined from the experimental frequency-response test on the X-15 and can be approximated by a simple first-order lag with a break frequency of 5.5 cps. The aircraft dynamic

characteristics were obtained from the rolling-moment equation for zero dynamic pressure and yaw rate.

The method for reducing or eliminating the response of the system to the 13 cps structural vibration was to attenuate the output of the shaping network such that the signal level is always within the valve dead band at this frequency. Such attenuation is easily accomplished, as a result of the saturating-amplifier characteristics. Since the gyro output is limited to 5 deg/sec, an attenuation level of one-fifth, or approximately 14 decibels, would be sufficient for a minimum dead-band setting of 1 deg/sec. Various combinations of shaping that would exhibit this characteristic at 13 cps were mechanized on an analog computer. It was found that adequate results could be obtained by using a second-order filter with a natural frequency of 3 cps and a damping ratio of 0.5.

The response characteristics from the gyro input to the shaping network output are shown in figure 22(a) for the production shaping and in figure 22(b) for the modified shaping. For the production shaping, the response is essentially flat out to 23 cps, which corresponds to the natural frequency of the gyros. The phase crossover point is at about 25 cps. For the second-order shaping with a natural frequency of 3 cps and a damping ratio of 0.5, the response begins to fall off at about 3 cps. At 13 cps, the attenuation level is down to 20 decibels, which insures that the output signal will always fall within the control-valve dead band. Thus, the valve will be prevented from operating at the 13 cps structural resonant frequencies. Because of the additional phase lag added to the system by the modified shaping, the phase crossover point occurs at about 8 cps.

Total open-loop response characteristics before and after the filter modification are compared in figure 23. The low-frequency response is essentially the same for the two types of shaping up to about 3 cps. The amplitude response of the modified shaping drops off sharply at about 2 cps and becomes asymptotic to a frequency of about 12.5 cps, indicating that no output is obtained above this frequency.

The difference in the phase-angle characteristics for the two shapings can be seen from the dashed and solid lines. As shown by the dashed lines, the 180° crossover point for the production shaping is at about 3.6 cps and was decreased to 2.2 cps with the addition of the modified shaping. Although this increased lag is a significant addition to the total phase-lag characteristics, it is not believed to be restrictive, because of the inertial characteristics of the vehicle and its response in the low-dynamic-pressure flight regions.

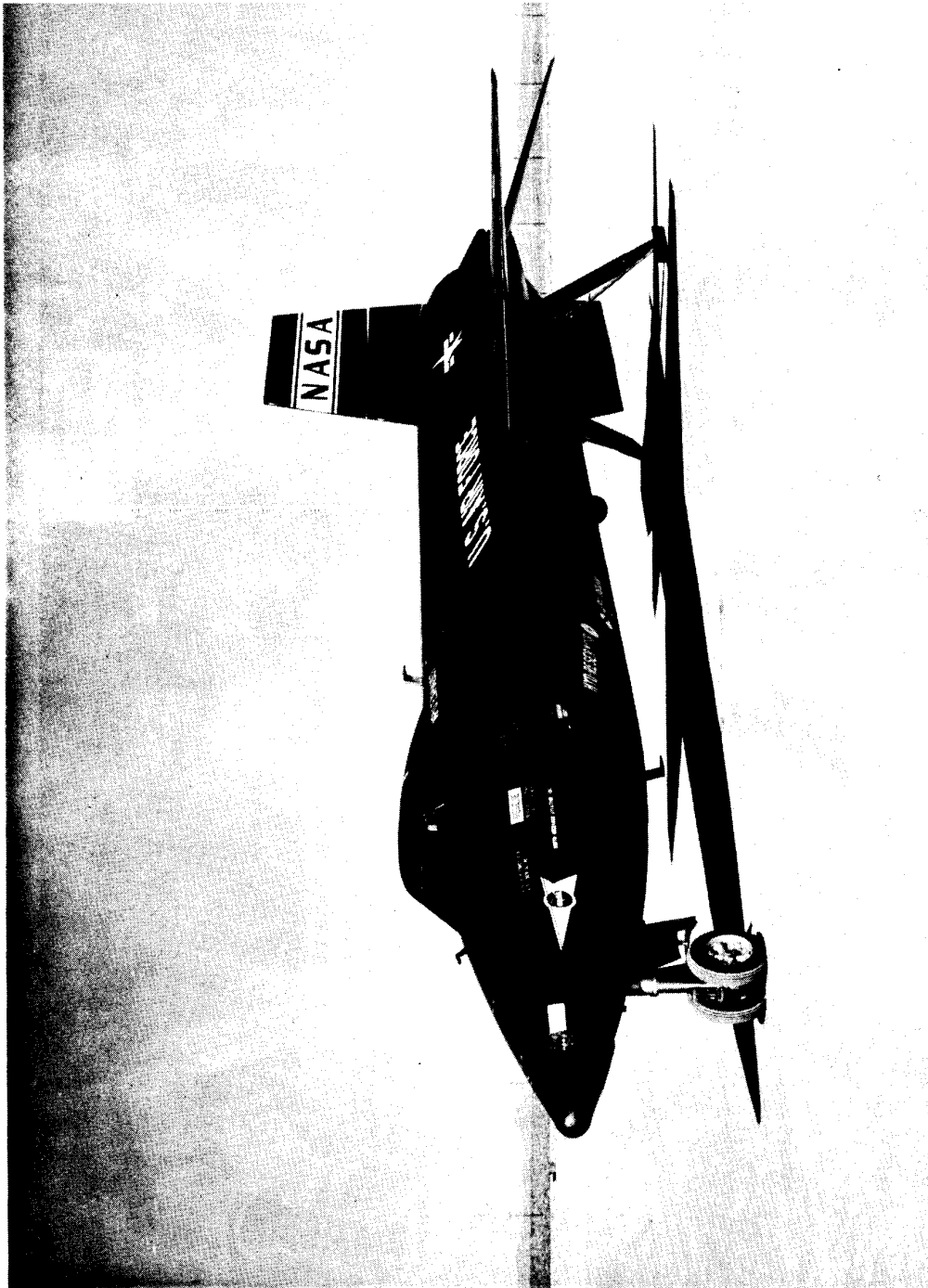
## REFERENCES

1. Jarvis, Calvin R.; and Adkins, Elmor J.: Operational Experience with X-15 Reaction Controls. [Preprint] 857G, SAE-ASME, Apr. 27-30, 1964.
2. Holleman, Euclid C.; and Adkins, Elmor J.: Contributions of the X-15 Program to Lifting Entry Technology. J. Aircraft, vol. 1, no. 6, Nov.-Dec. 1964, pp. 360-366.
3. Stillwell, Wendell H.; and Drake, Hubert M.: Simulator Studies of Jet Reaction Controls for Use at High Altitude. NACA RM H58G18a, 1958.
4. Holleman, Euclid C.; and Stillwell, Wendell H.: Simulator Investigation of Command Reaction Controls. NACA RM H58D22, 1958.
5. Farr, E. J.: Analog Simulation Studies of a Reaction Control Augmentation System for the X-15 Research Airplane. Rep. NA-60-1066, North American Aviation, Inc., Nov. 23, 1960.
6. Cooper, George E.: Understanding and Interpreting Pilot Opinion. Aeron. Eng. Rev., vol. 16, no. 3, Mar. 1957, pp. 47-51, 56.
7. Besco, R. O.; Depolo, G. G.; and Bauerschmidt, D. K.: Manual Attitude Control Systems: Parametric and Comparative Studies of Operating Modes of Control. NASA CR-56, 1964.
8. Petersen, Forrest S.; Rediess, Herman A.; and Weil, Joseph: Lateral-Directional Control Characteristics of the X-15 Airplane. NASA TM X-726, 1962.
9. Love, James E.; and Stillwell, Wendell H.: The Hydrogen-Peroxide Rocket Reaction-Control System for the X-1B Research Airplane. NASA TN D-185, 1959.
10. Reisert, Donald; and Adkins, Elmor J.: Flight and Operational Experiences With Pilot Operated Reaction Controls. ARS J., vol. 32, no. 4, Apr. 1962, pp. 626-631.
11. Taylor, Lawrence W., Jr.; and Merrick, George B.: X-15 Airplane Stability Augmentation System. NASA TN D-1157, 1962.

TABLE I

## X-15 ATTITUDE CONTROL ROCKET DESIGN AND PERFORMANCE PARAMETERS

	<u>Type A</u>	<u>Type B</u>
Chamber convergent half angle, deg . . . . .	45	-----
Chamber throat:		
Outside radius, in. . . . .	0.500	0.188
Inside diameter, in. . . . .	0.530	0.676
Area, sq in. . . . .	0.221	0.100
Diameter, in. . . . .	1.600	-----
Nozzle:		
Exit area, sq in. . . . .	2.074	1.227
Divergent half angle, deg . . . . .	18	23
Contour radius, in. . . . .	-----	2.545
Pintle:		
Contour radius, in. . . . .	-----	2.545
Half angle, deg . . . . .	-----	23
Diameter, in. . . . .	-----	0.574
Length (throat and tip), in. . . . .	-----	0.843
Area ratio, sq in. . . . .	9.401	12.260
Pressure ratio $\left(\frac{P_c}{P_e}\right)$ for full flow . . . . .	87.681	126.36
Rocket thrust coefficient (h = 200,000 ft) . . . . .	1.67	1.65
Thrust (h = 200,000 ft), lb . . . . .	113 ±6	43 ±3
Rated feed pressure, psia . . . . .	420	390
Rated chamber pressure, psia . . . . .	307	265
Nominal rated flow, lb/sec . . . . .	0.715	0.27
Characteristic exhaust velocity, ft/sec . . . . .	3030	3120
Total impulse, lb-min . . . . .	646	389
Specific impulse, minimum (h = 200,000 ft), sec. . . . .	159	156



E-7902

Figure 1.- X-15 airplane.

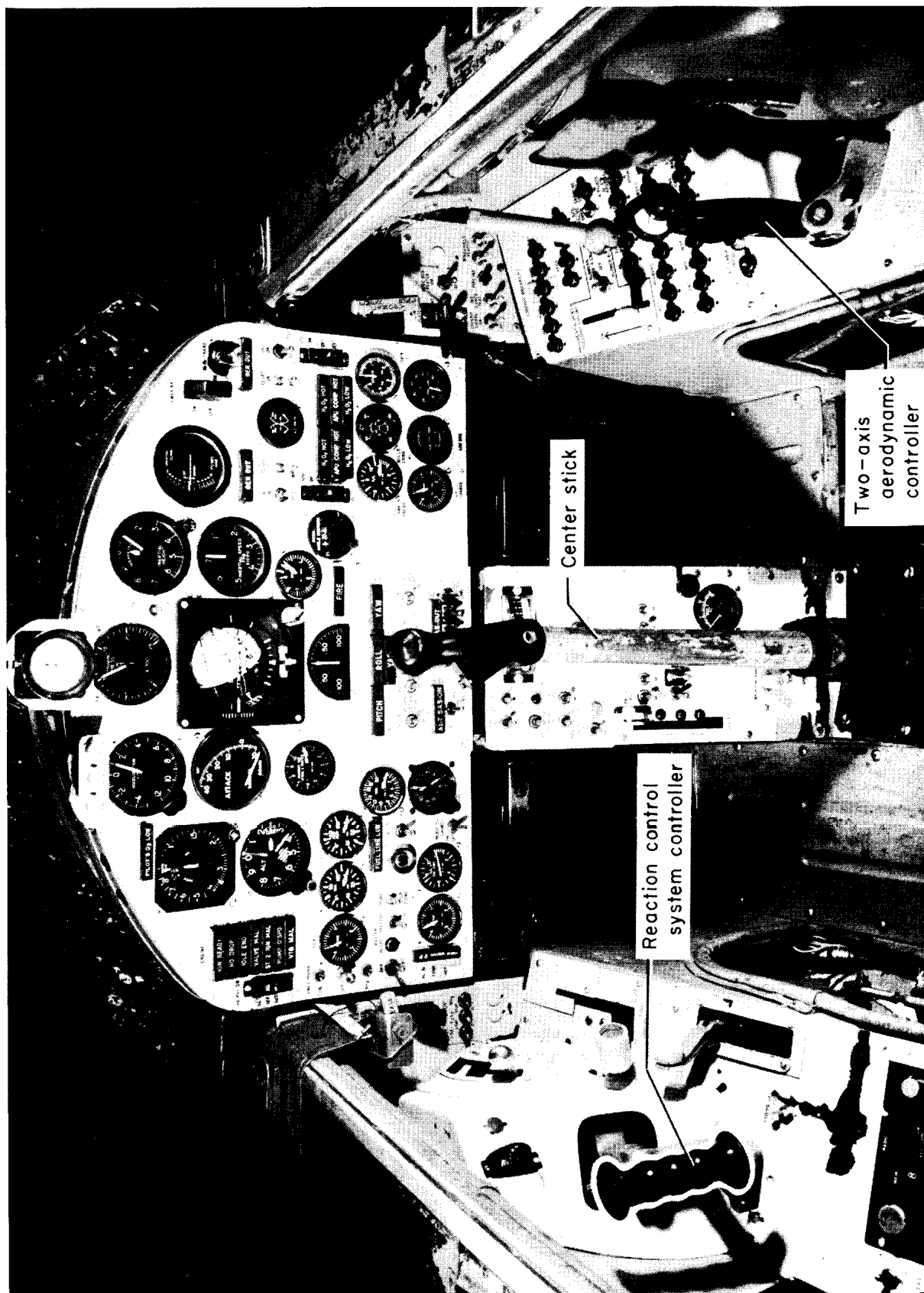


Figure 2.- X-15 cockpit.



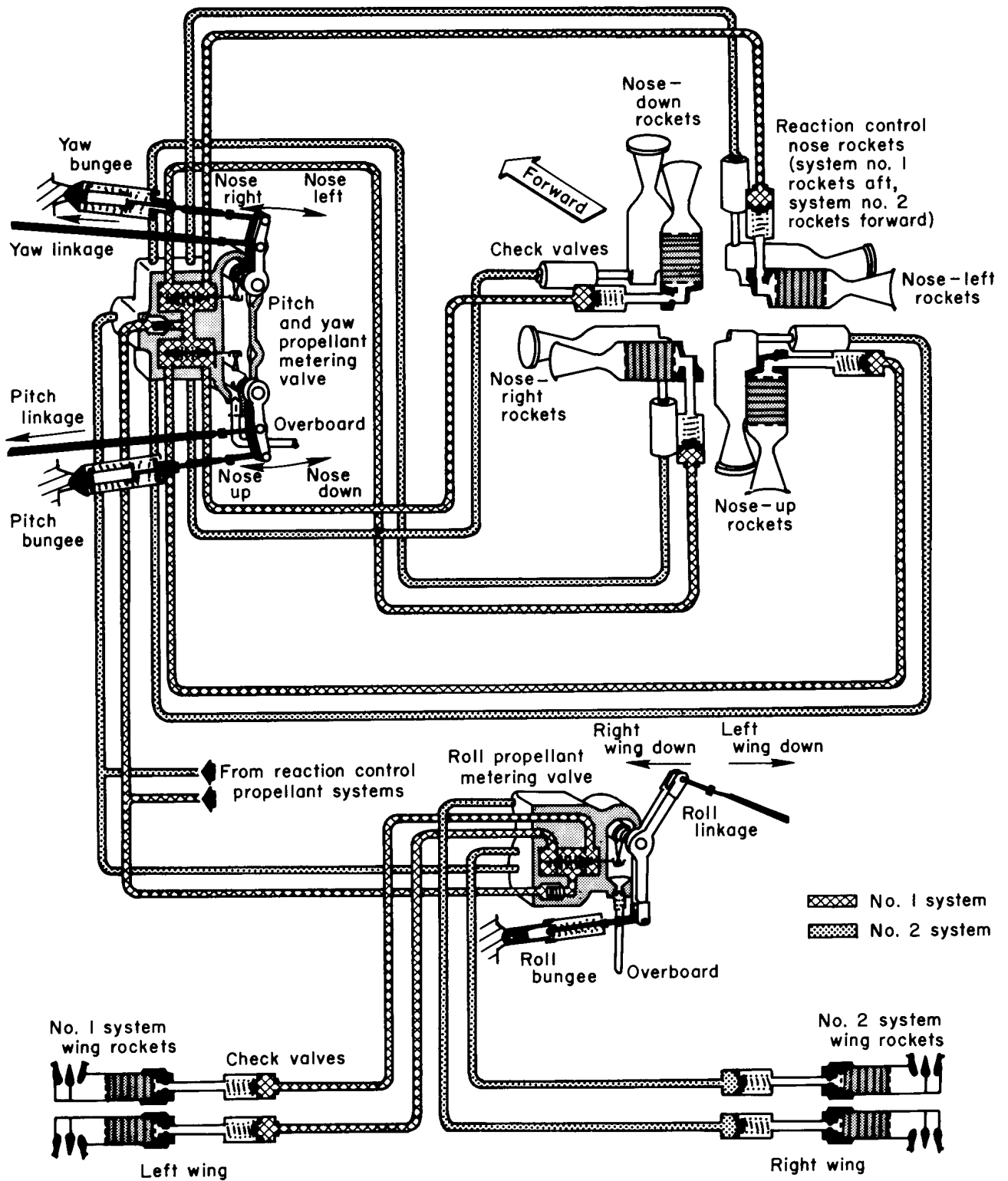


Figure 3.— Schematic diagram of X-15 manual reaction control system components.

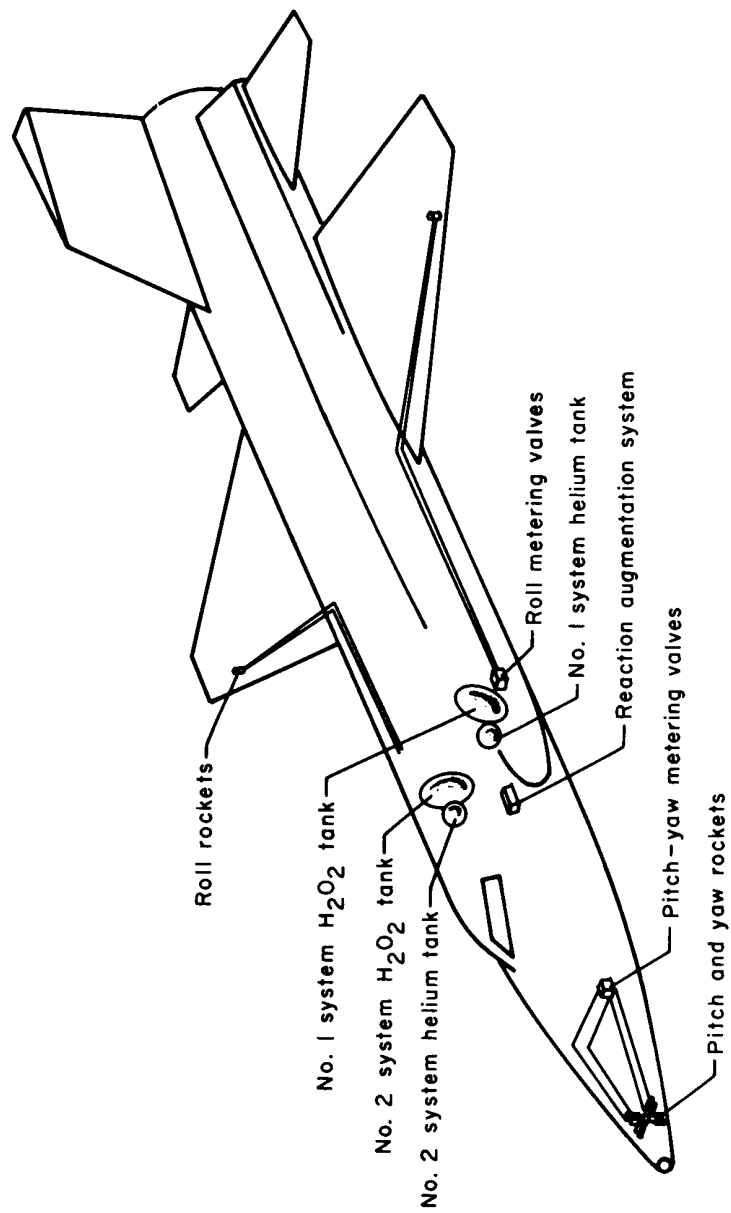


Figure 4.— Location of reaction control system components in X-15.

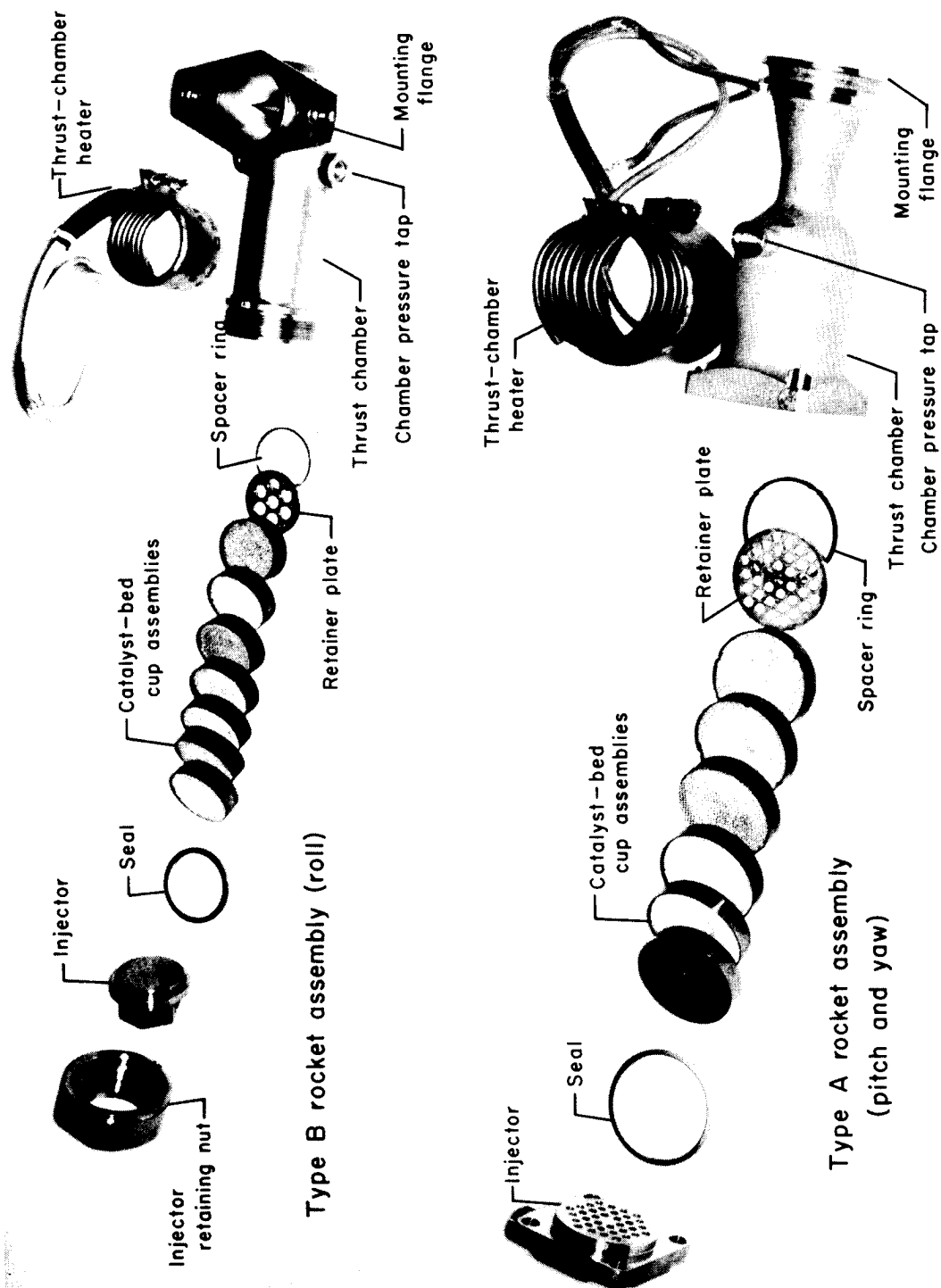


Figure 5.— Reaction control rocket assemblies.

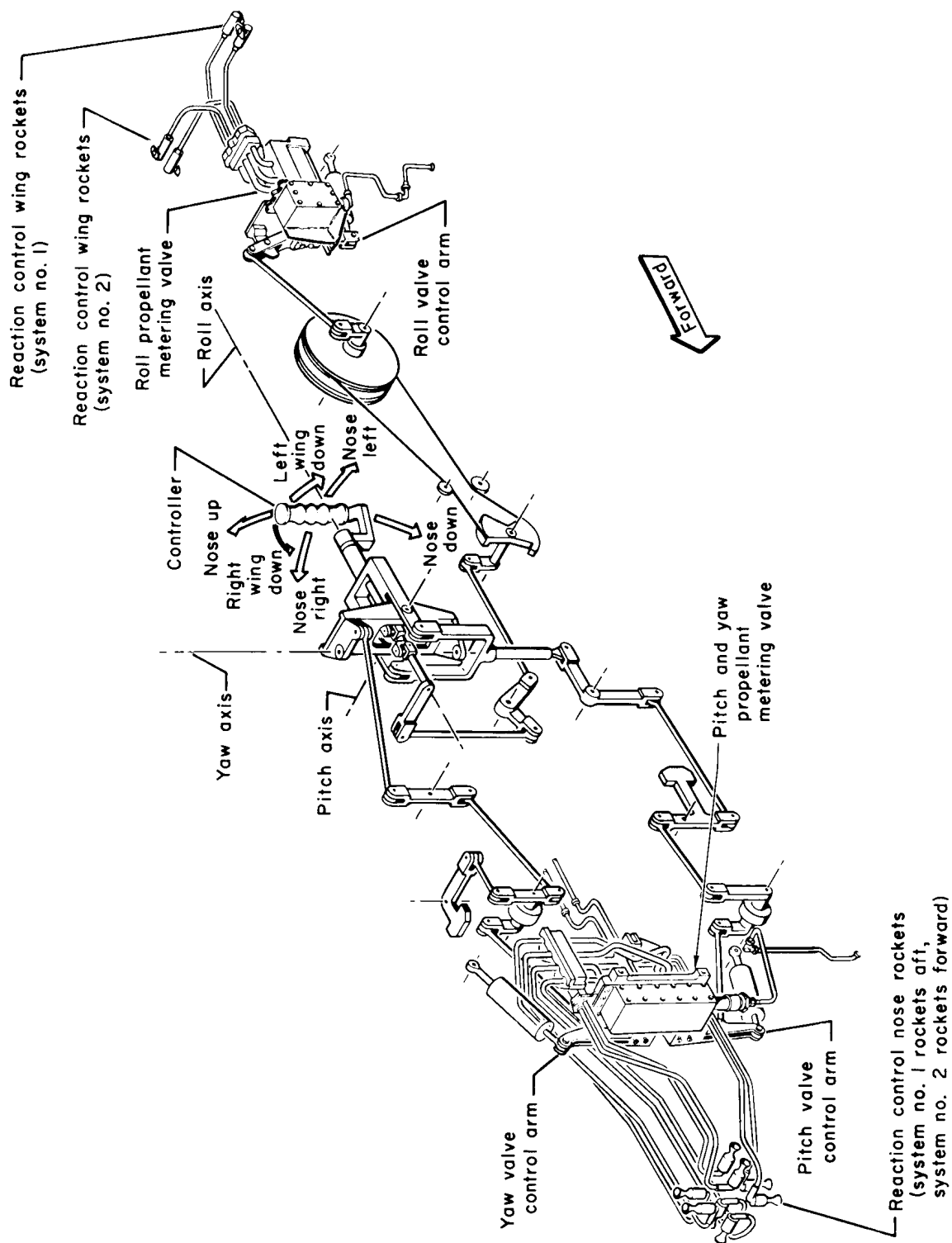


Figure 6.— Reaction control system mechanical linkage.

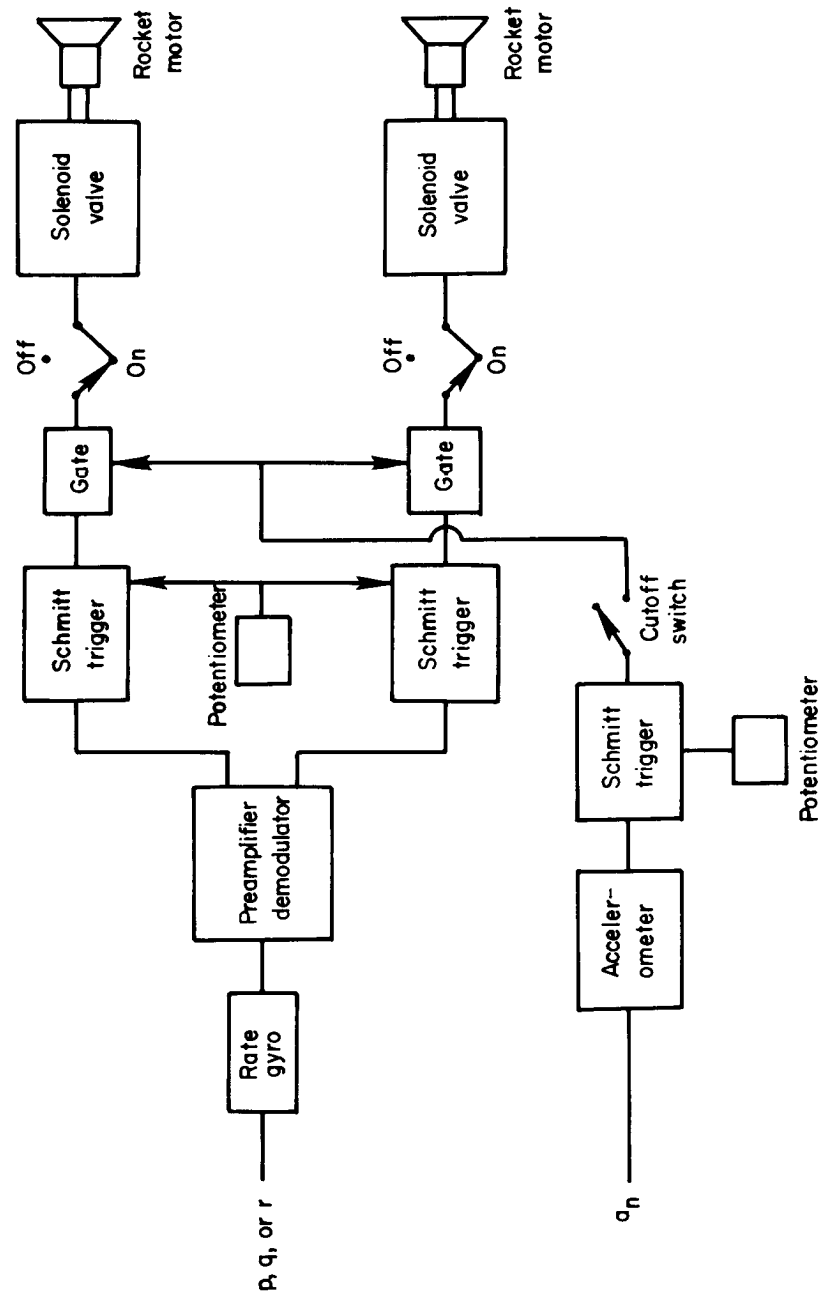


Figure 7.— Simplified block diagram showing one axis of the X-15 reaction augmentation system and the accelerometer cutoff feature.

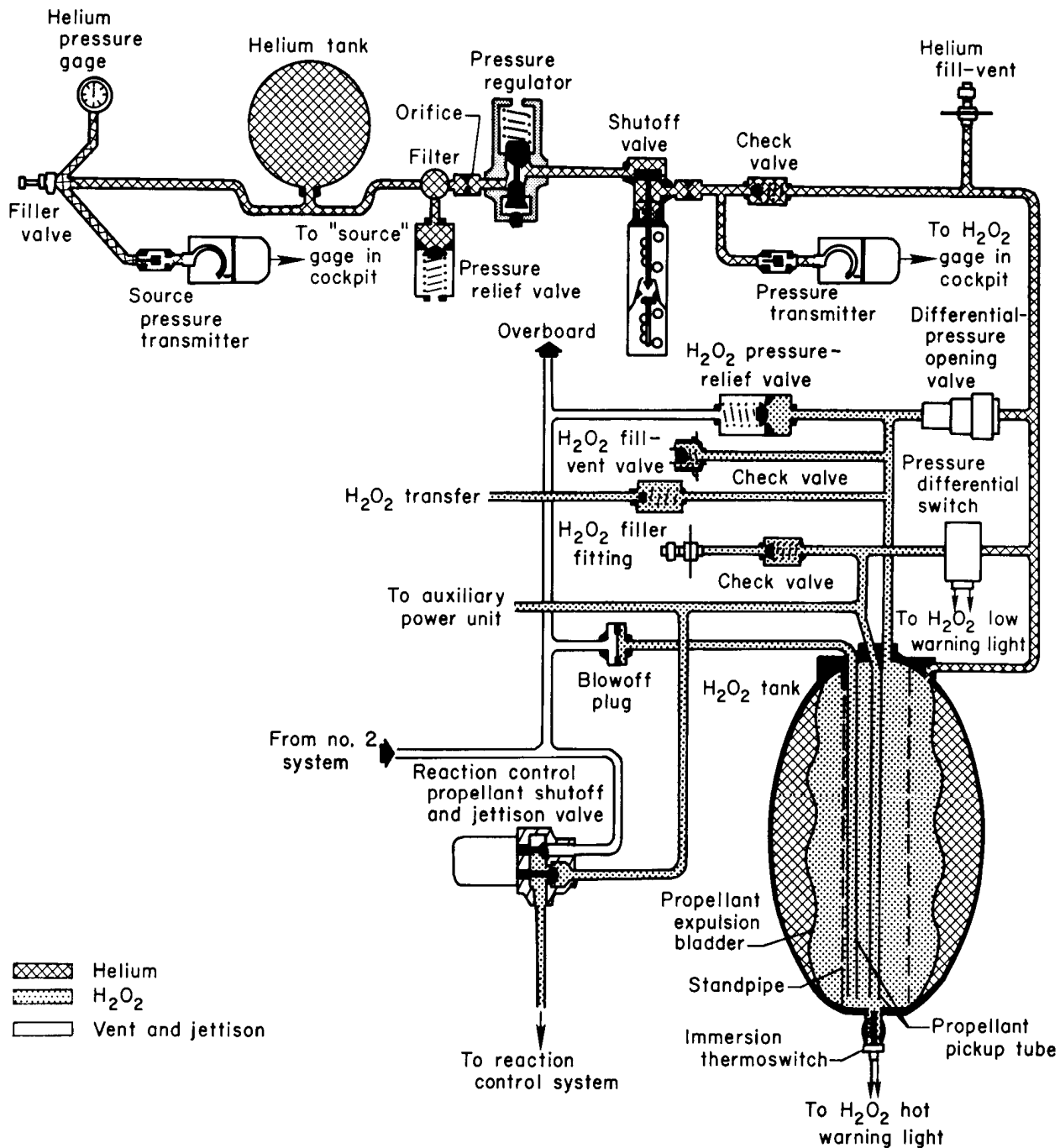
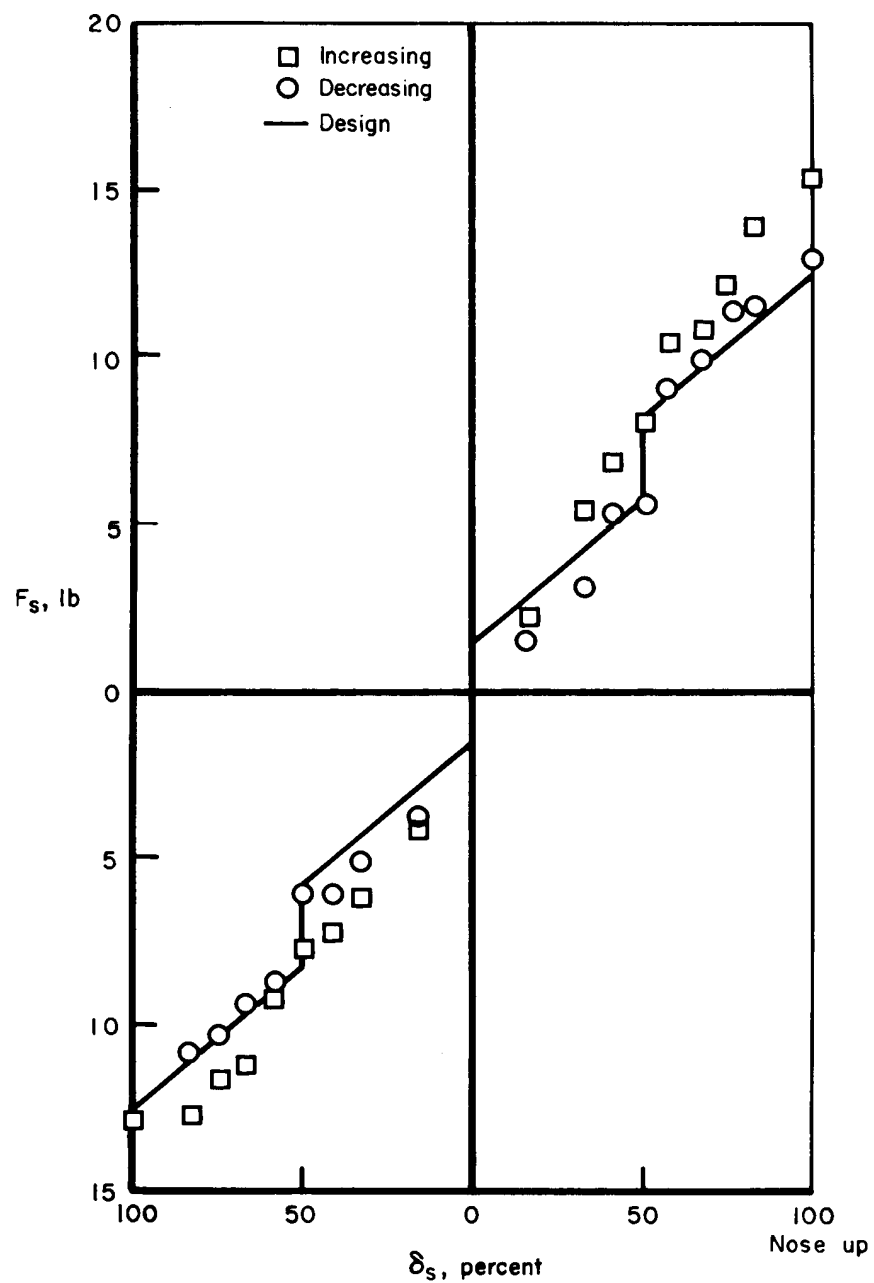
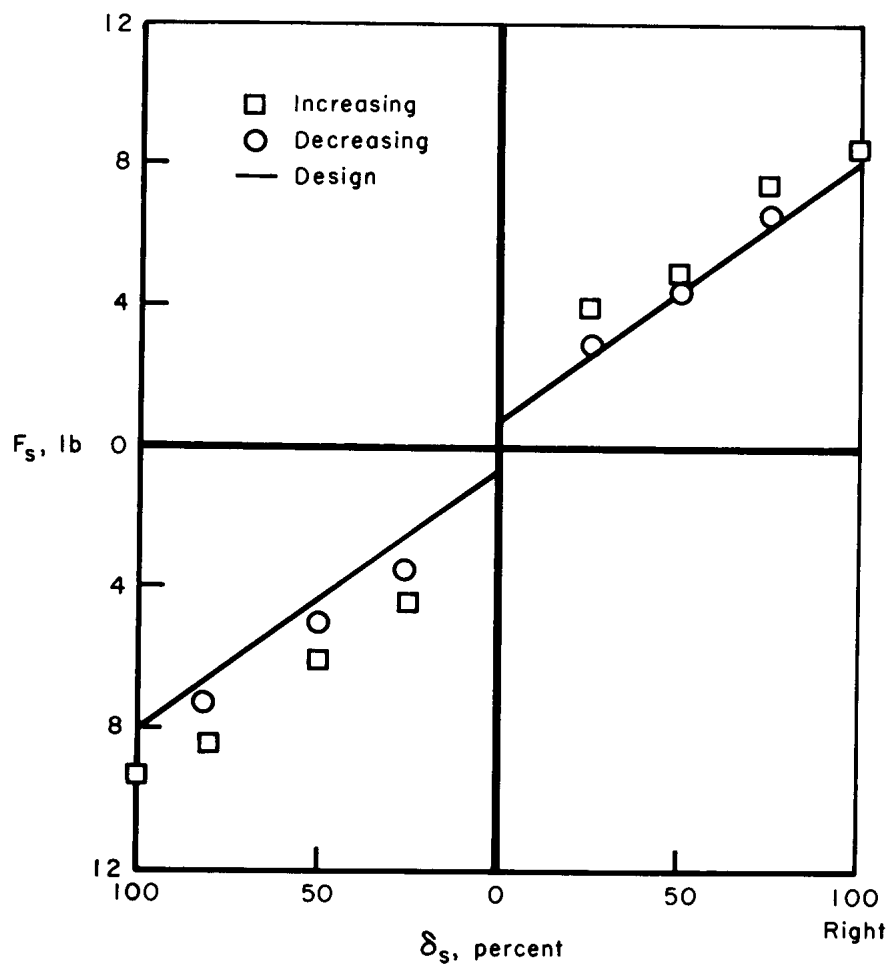


Figure 8.- X-15 reaction control propellant supply system (no. 1).



(a) Pitch axis; maximum  $\delta_s = \pm 9^\circ 47'$ .

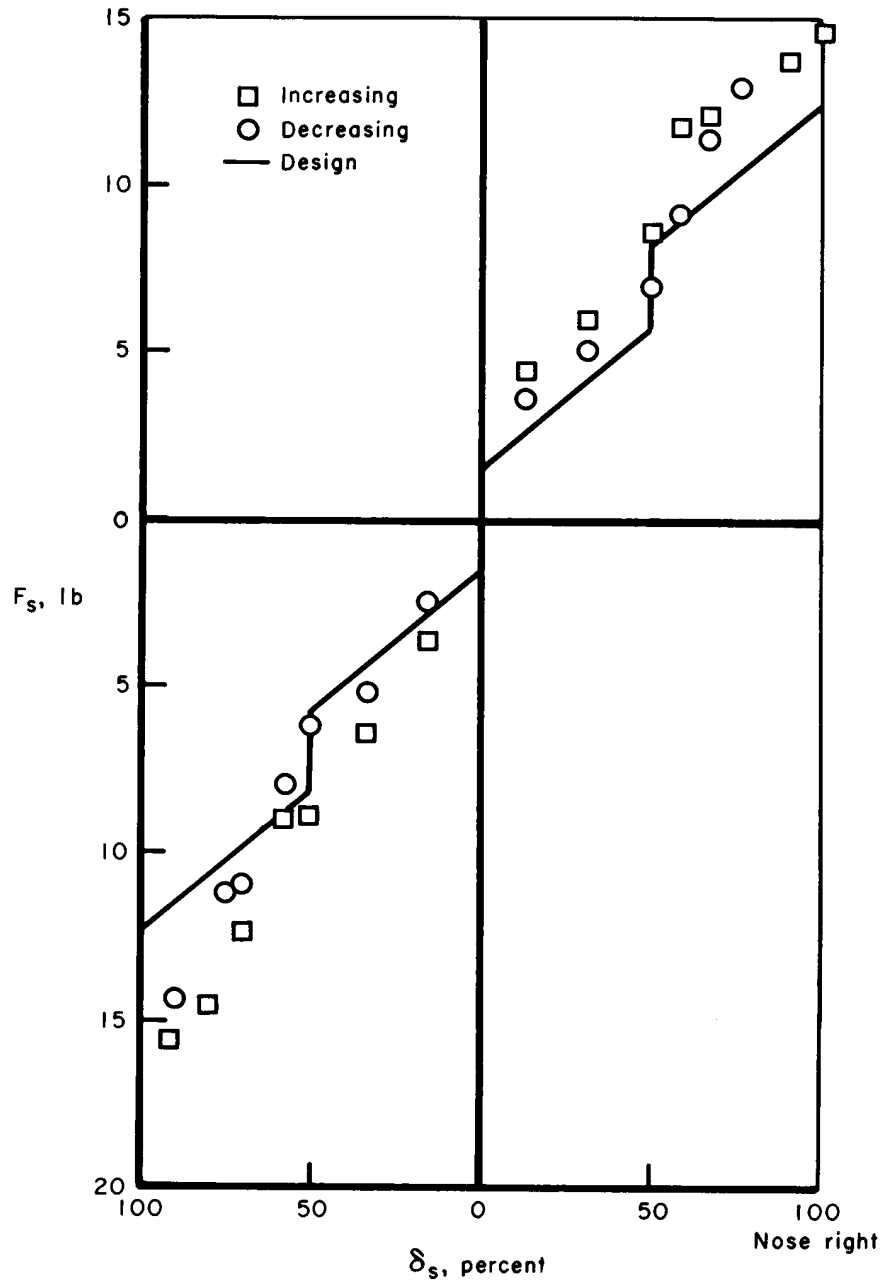
Figure 9.— Stick-force characteristics.



(b) Roll axis; maximum  $\delta_S = \pm 18^\circ$ .

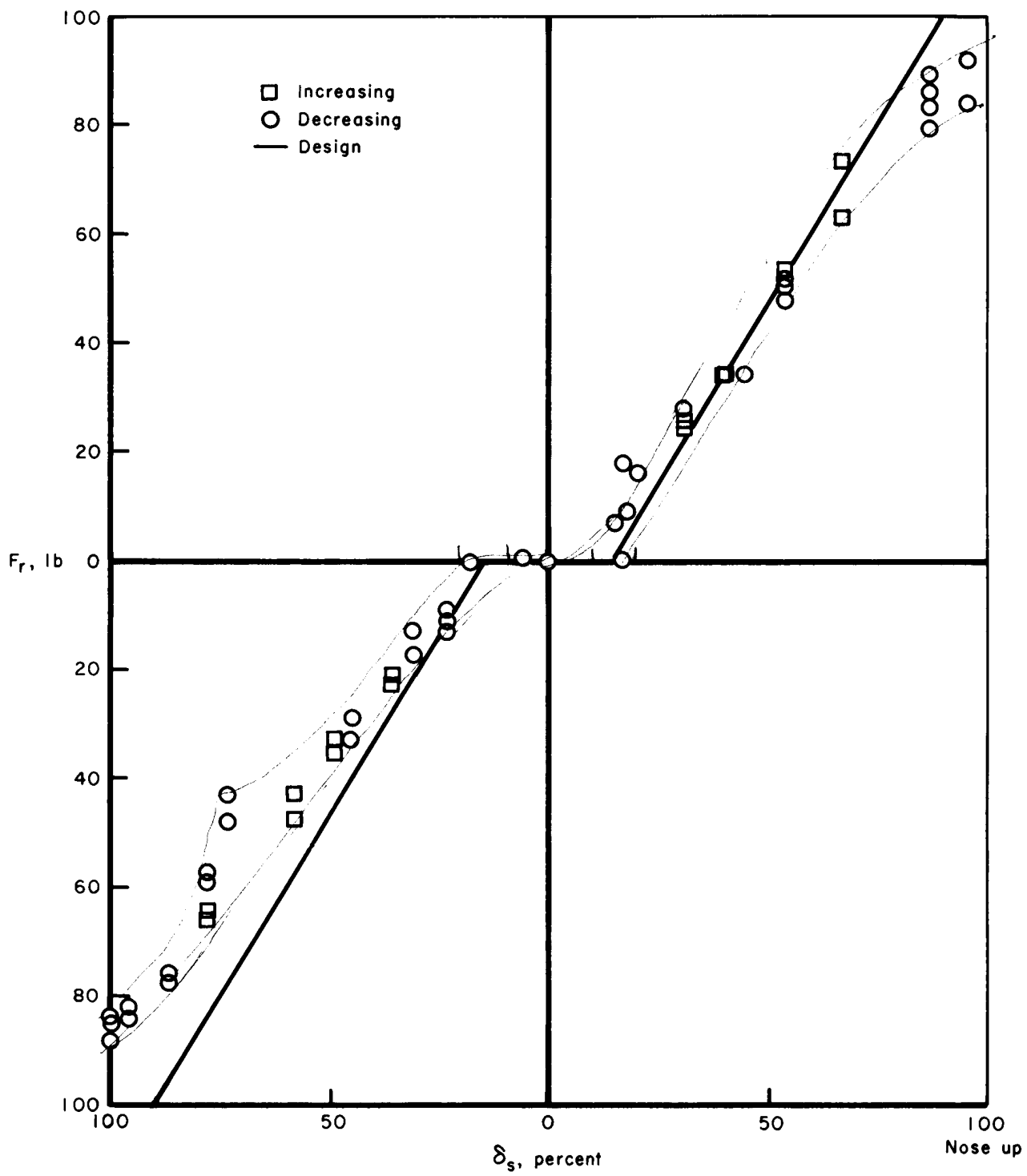
Figure 9.— Continued.





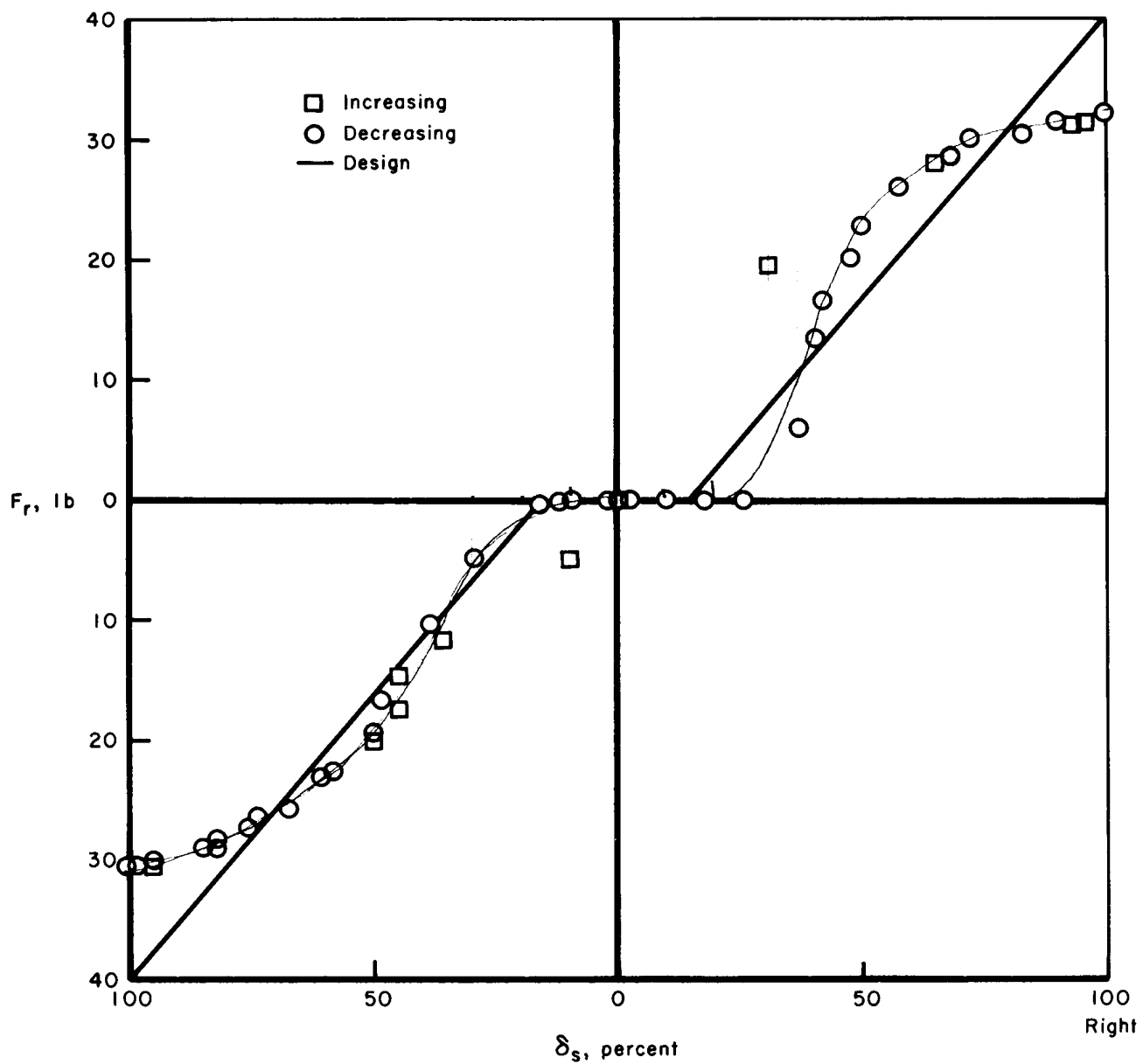
(c) Yaw axis; maximum  $\delta_s = \pm 8^\circ 2'$ .

Figure 9.— Concluded.



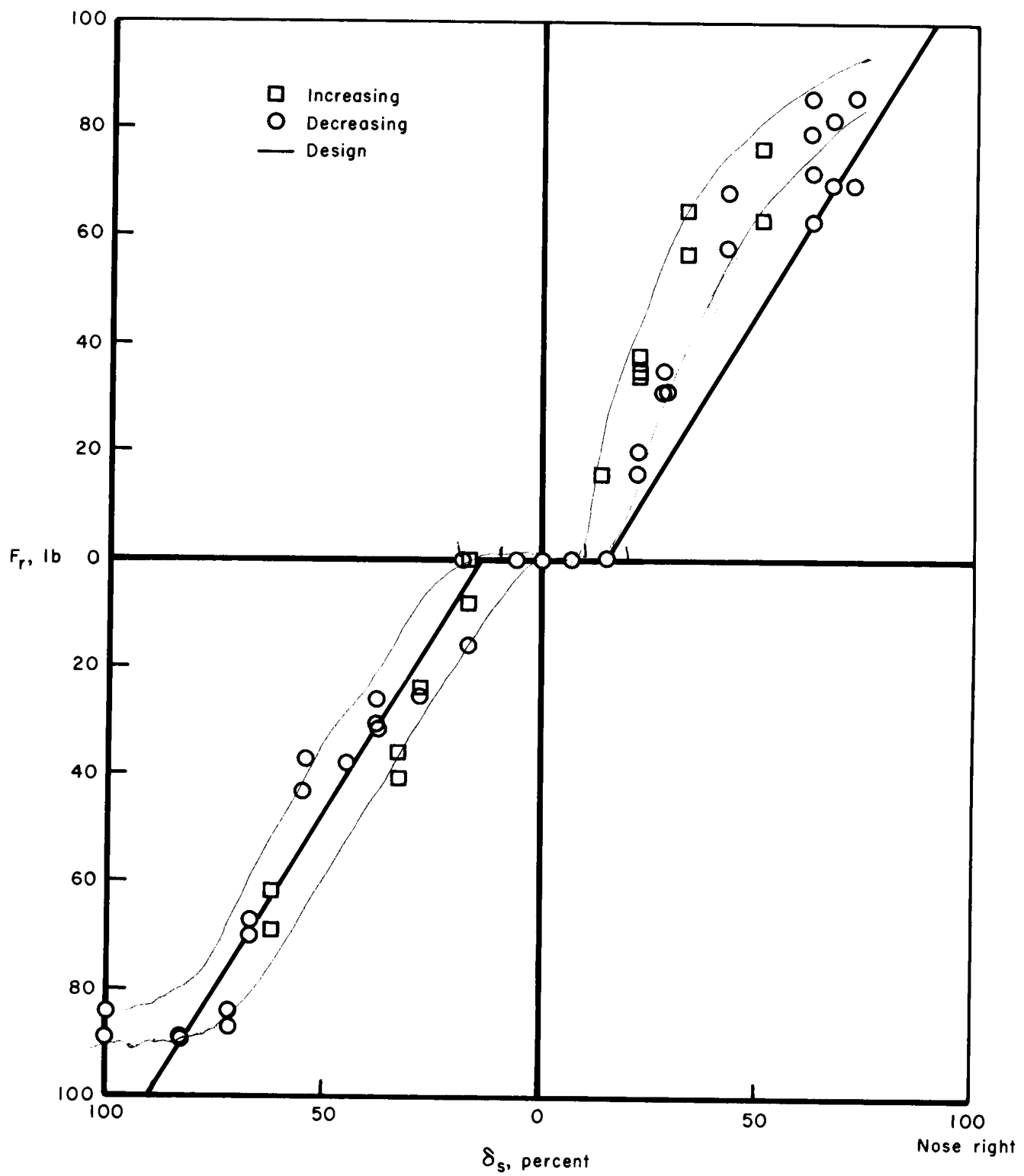
(a) Pitch axis; maximum  $\delta_s = \pm 9^\circ 47'$ .

Figure 10.— Reaction control rocket thrust as a function of controller deflection.



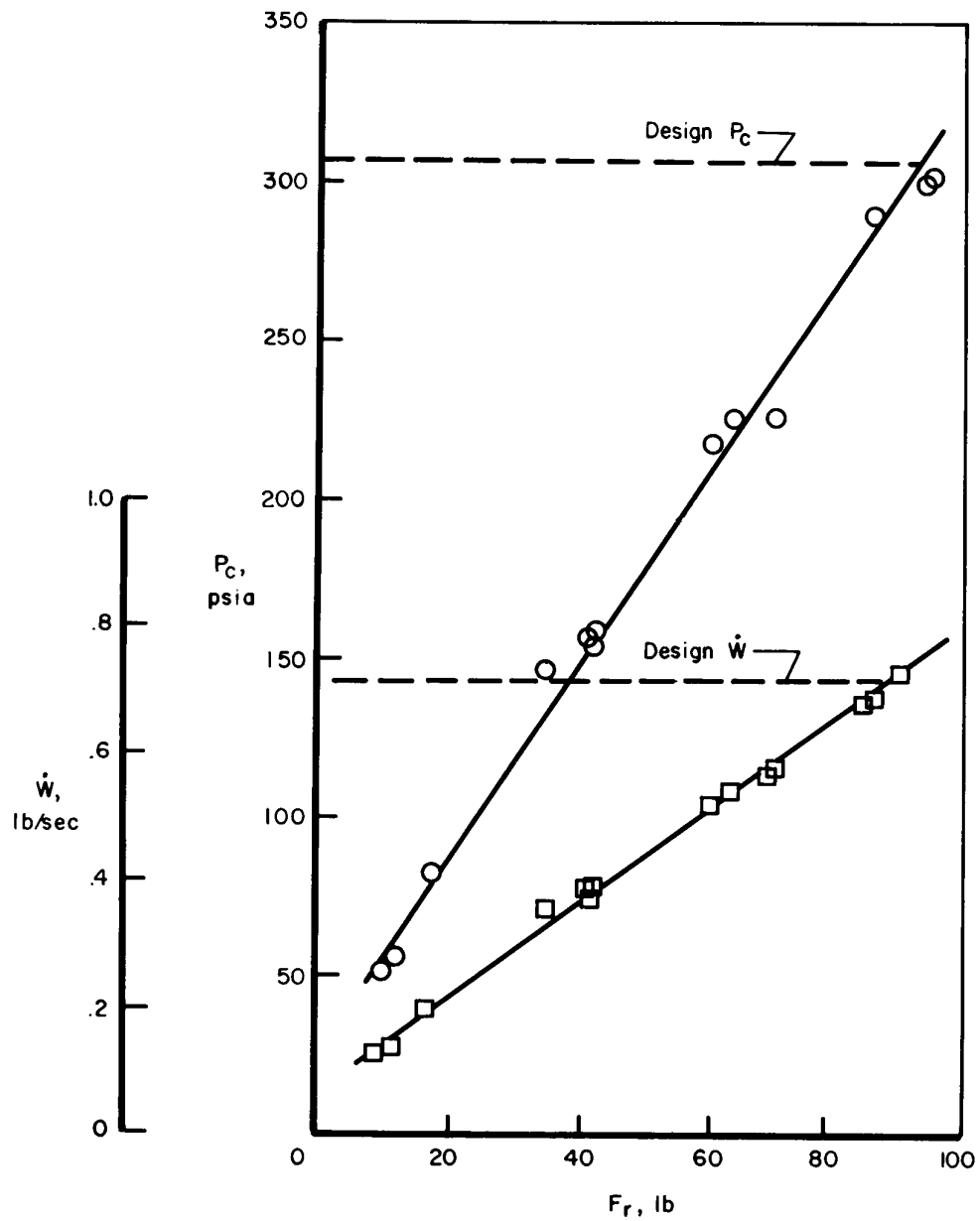
(b) Roll axis; maximum  $\delta_s = \pm 18^\circ$ .

Figure 10.— Continued.



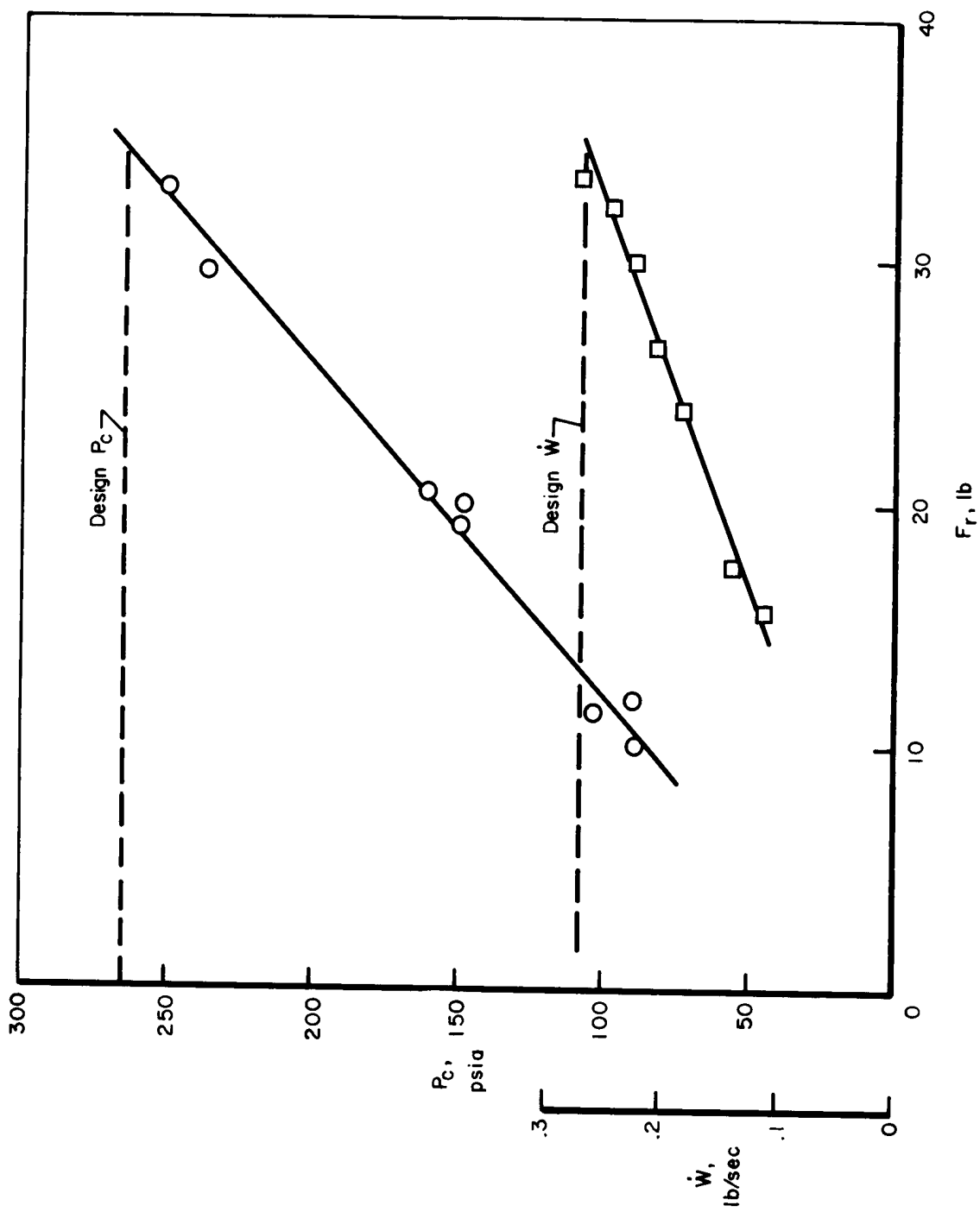
(c) Yaw axis; maximum  $\delta_s = \pm 8^\circ 2'$ .

Figure 10.— Concluded.



(a) Type A control rocket.

Figure 11.— Control rocket flow rate and chamber-pressure characteristics obtained from ground tests.



(b) Type B control rocket.

Figure 11.— Concluded.

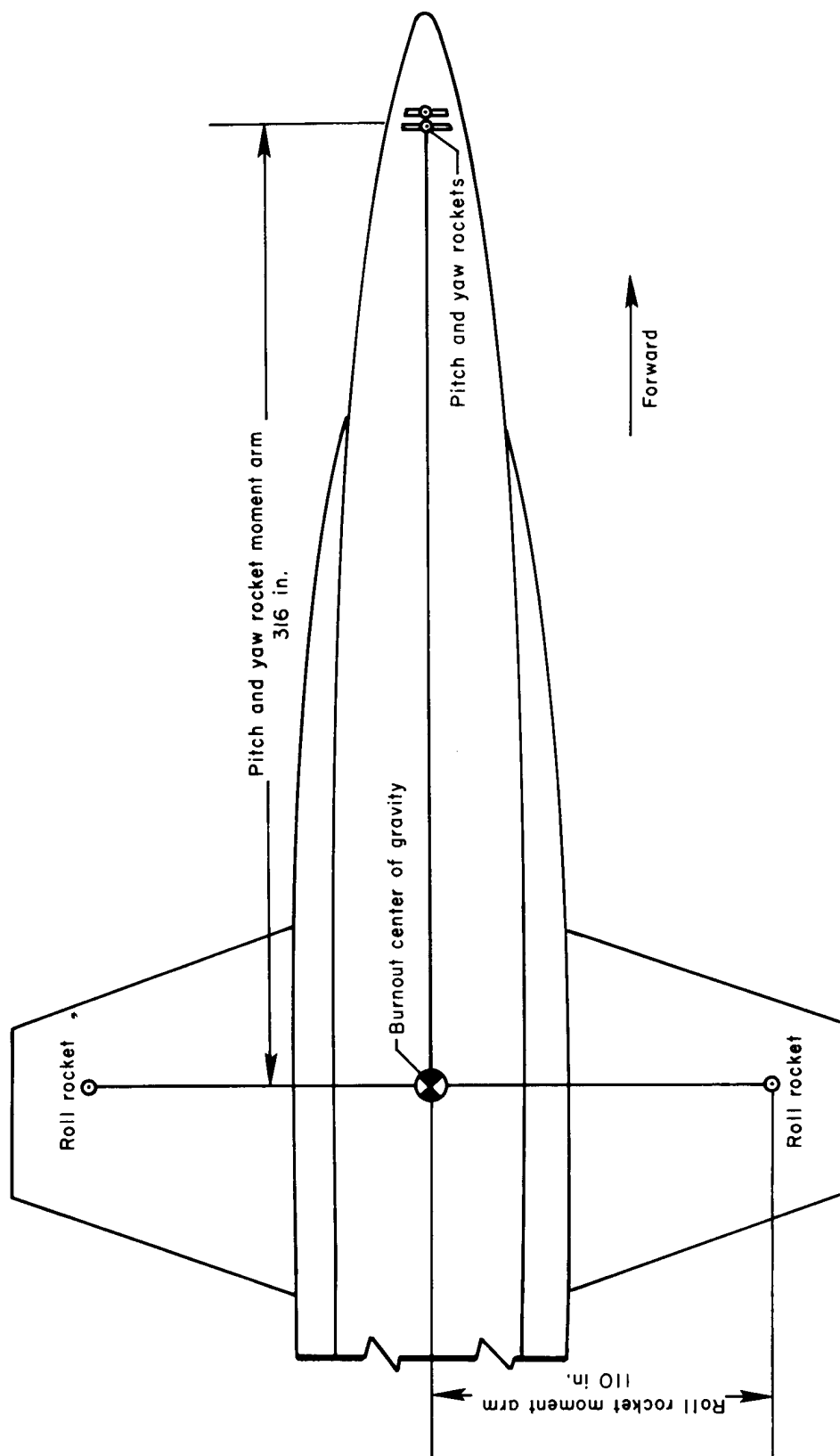


Figure 12.- Reaction control rocket locations and moment arms.

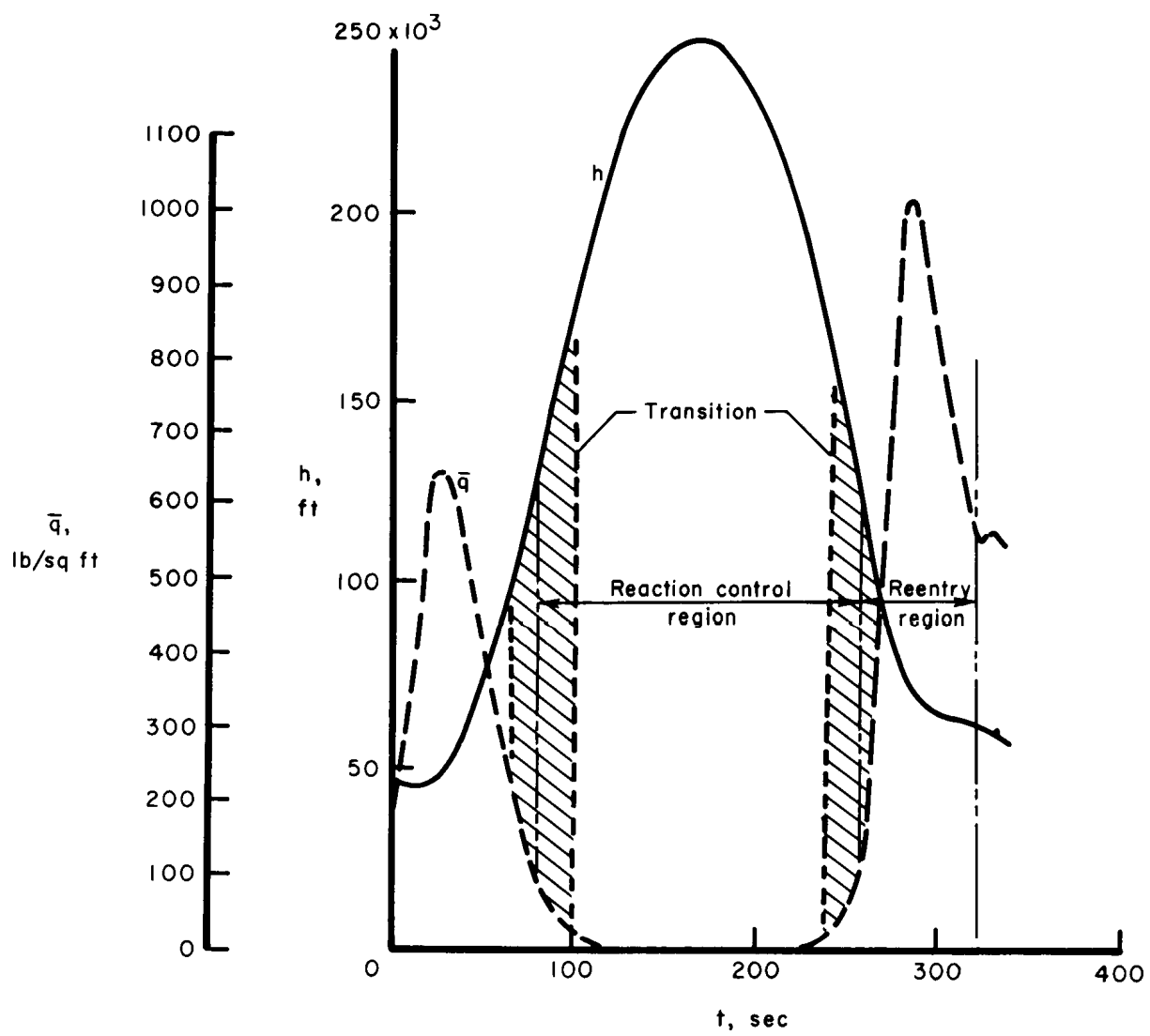


Figure 13.— Typical X-15 high-altitude-flight profile.



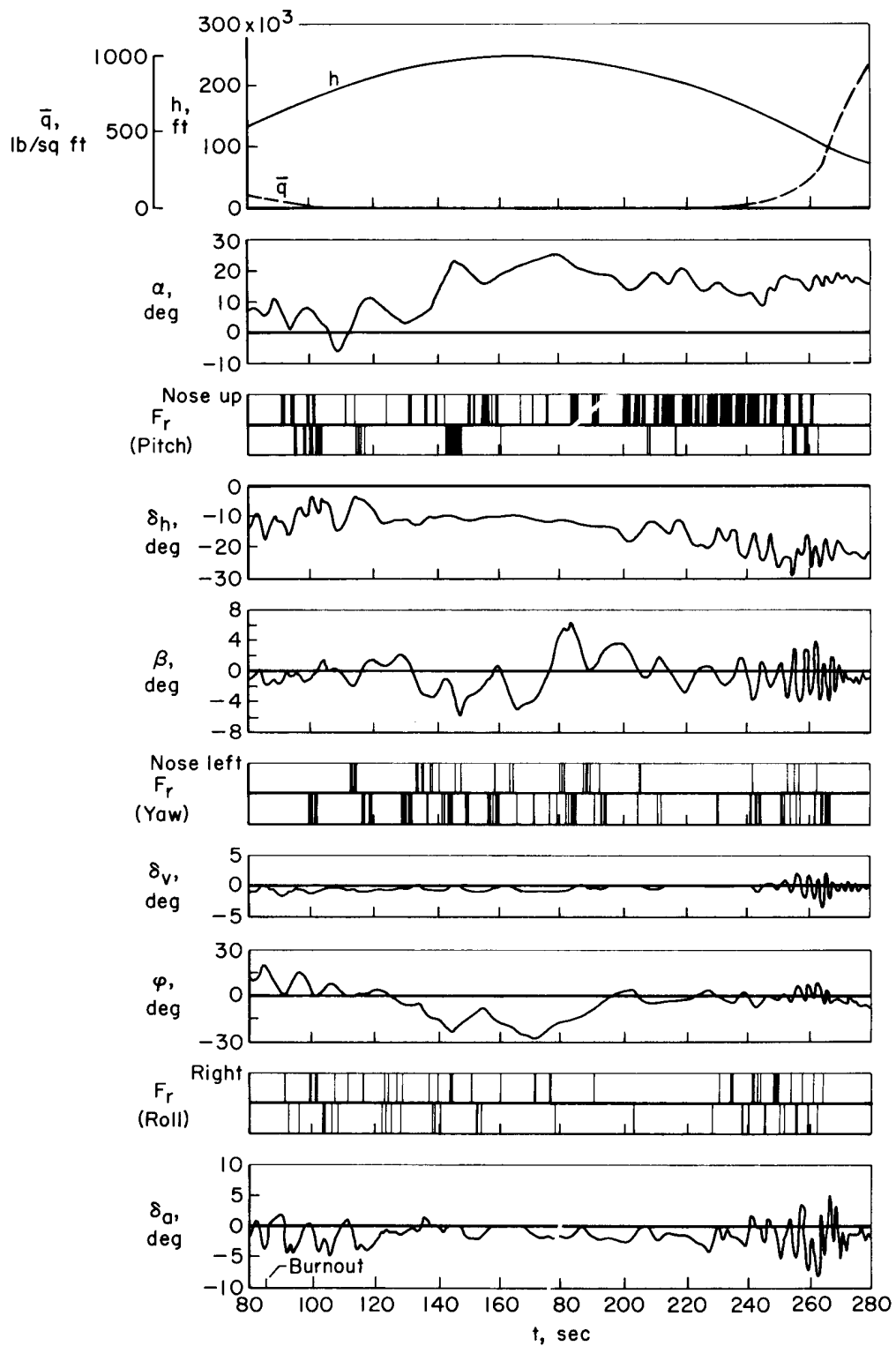


Figure 14.— Time history of reaction control portion of an X-15 high-altitude flight during which manual acceleration command system was used (time  $t$  referenced to launch).

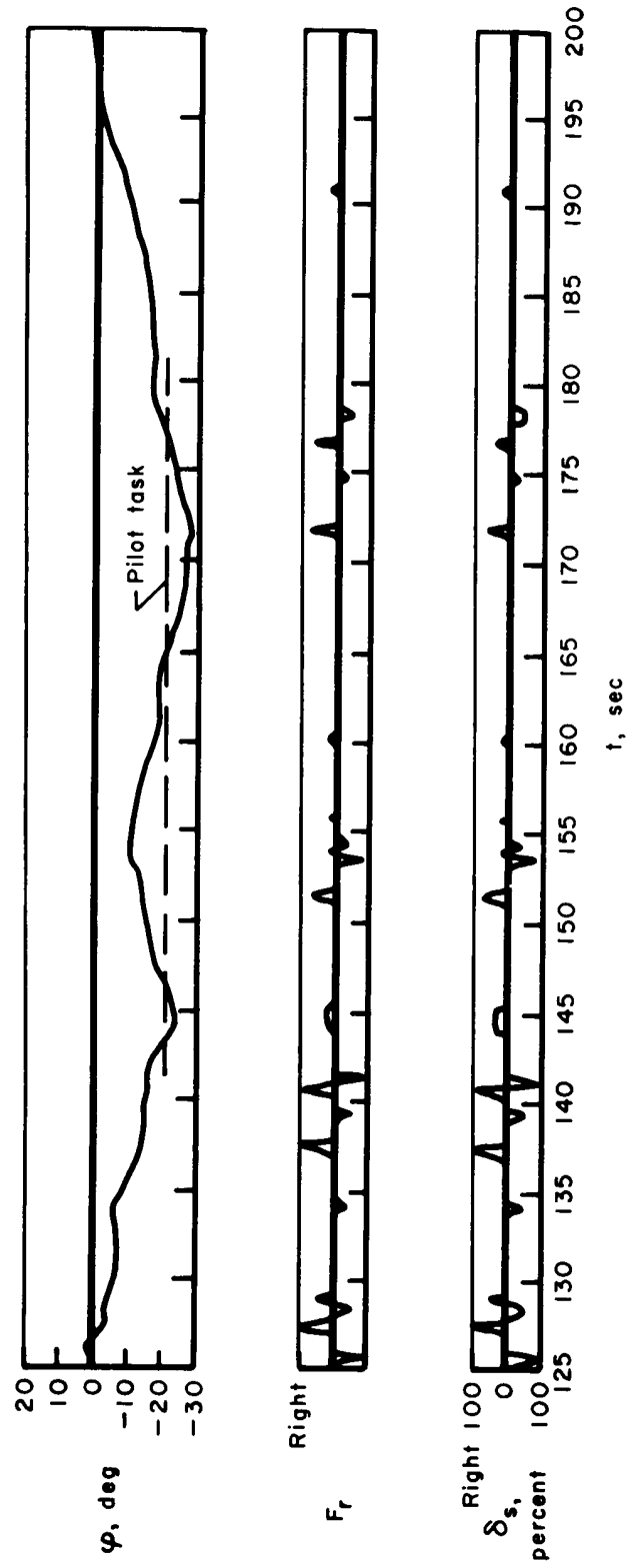


Figure 15.— Bank-angle maneuver using manual reaction controls (time  $t$  referenced to launch).

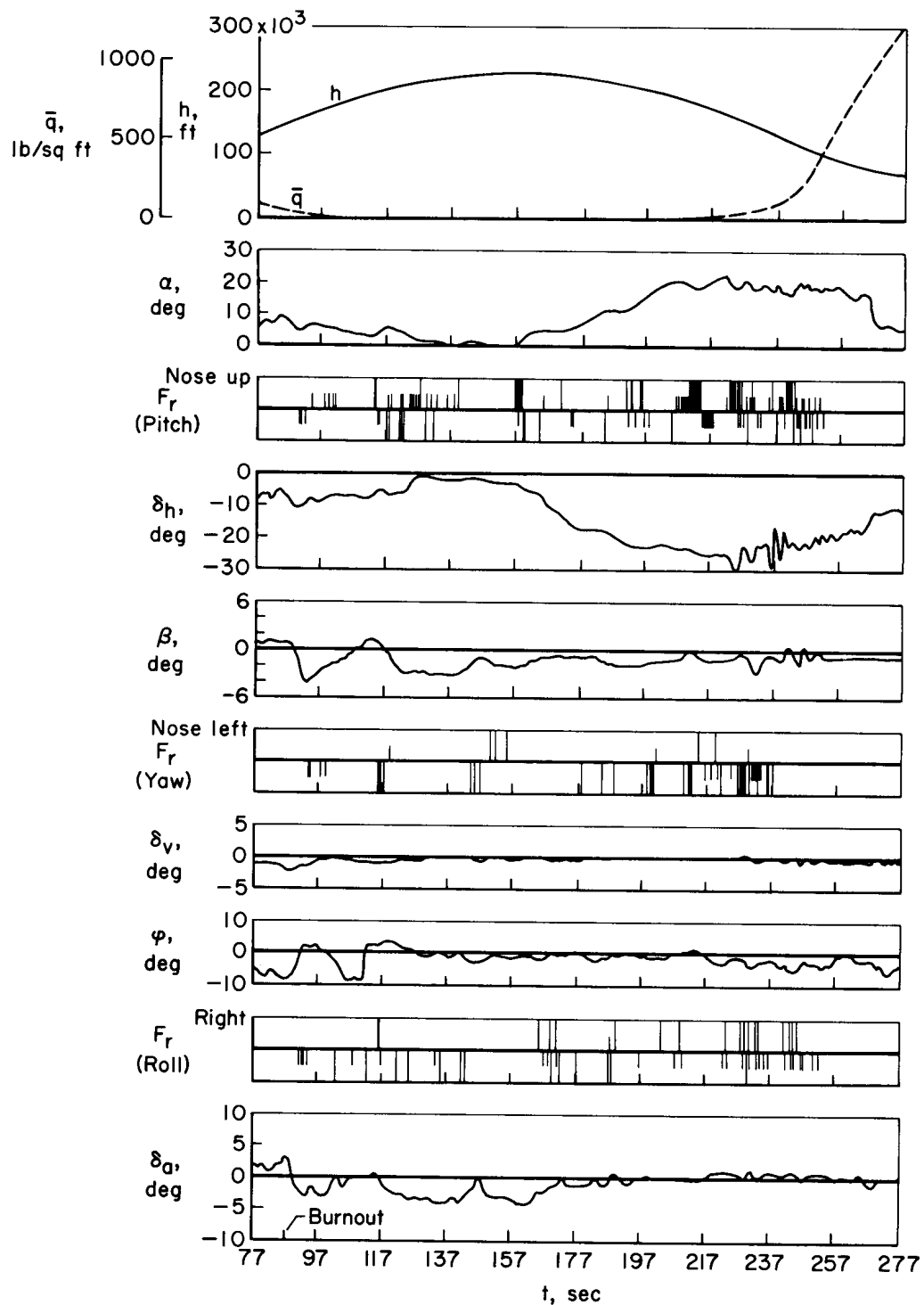


Figure 16.— Time history of a high-altitude X-15 flight during which both manual and reaction augmentation systems were used (time  $t$  referenced to launch).

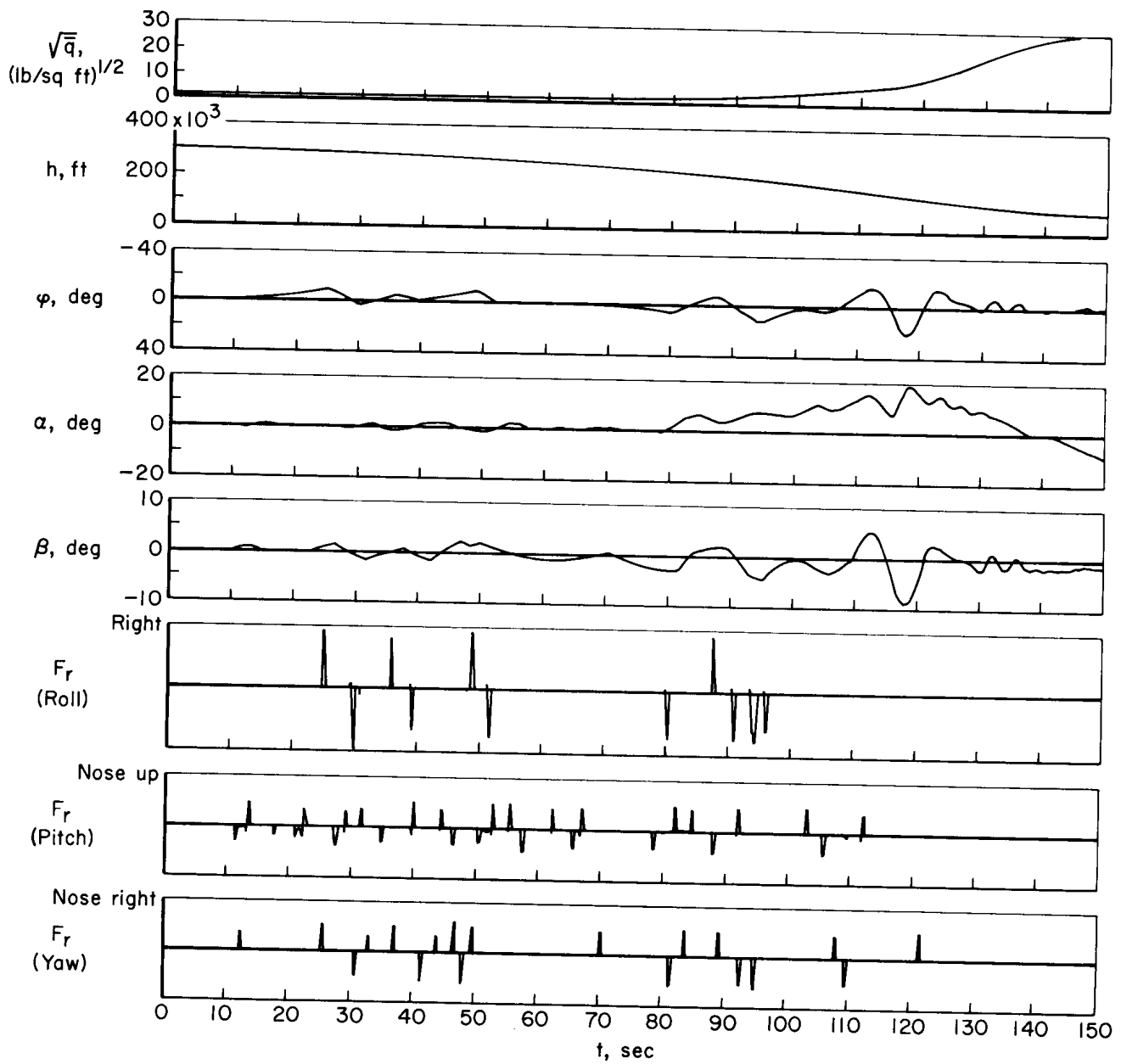


Figure 17.— X-15 manual acceleration command reentry made with six-degree-of-freedom flight simulator. Ventral-on configuration.

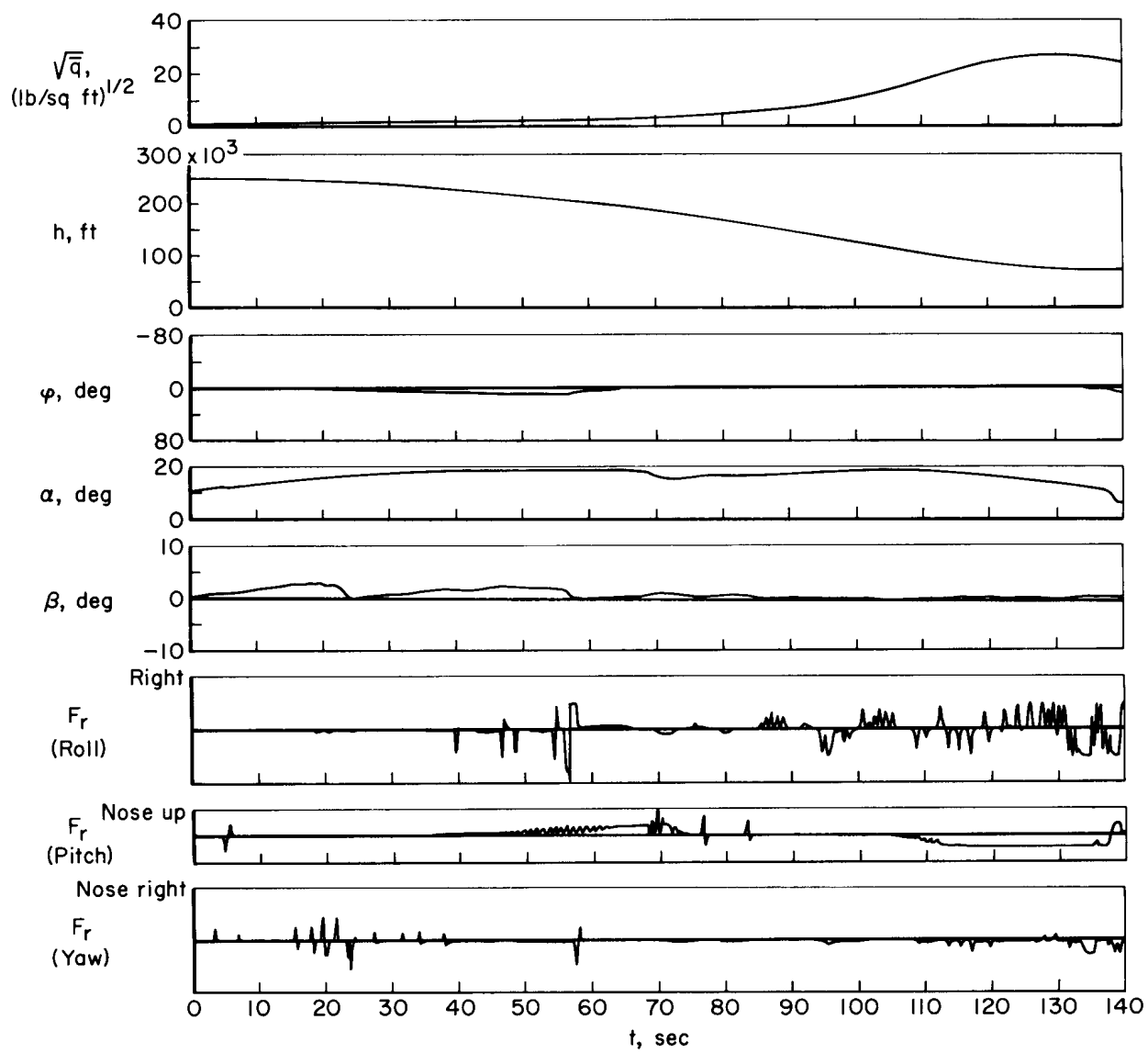


Figure 18.— X-15 reentry performed on a six-degree-of-freedom flight simulator using reaction control damping. Ventral-on configuration.

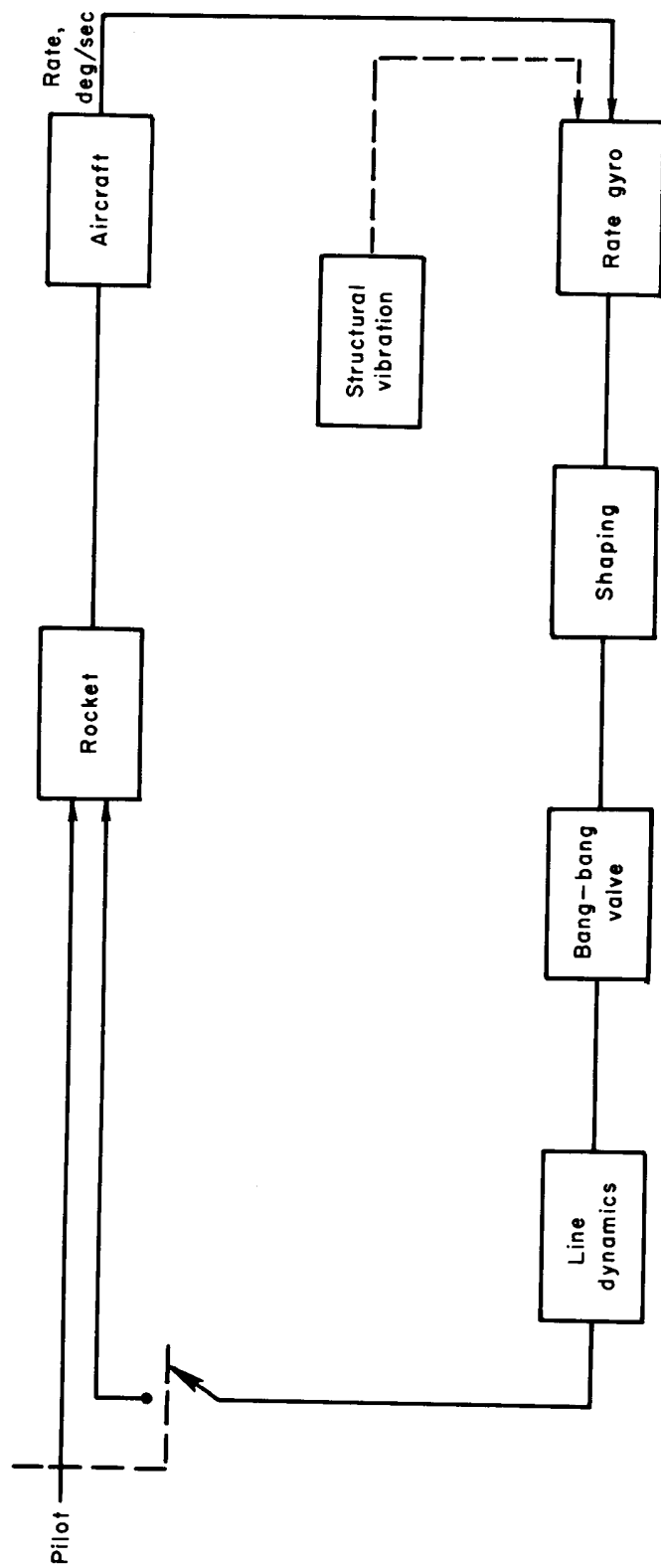


Figure 19.— Block diagram of X-15 reaction augmentation system.

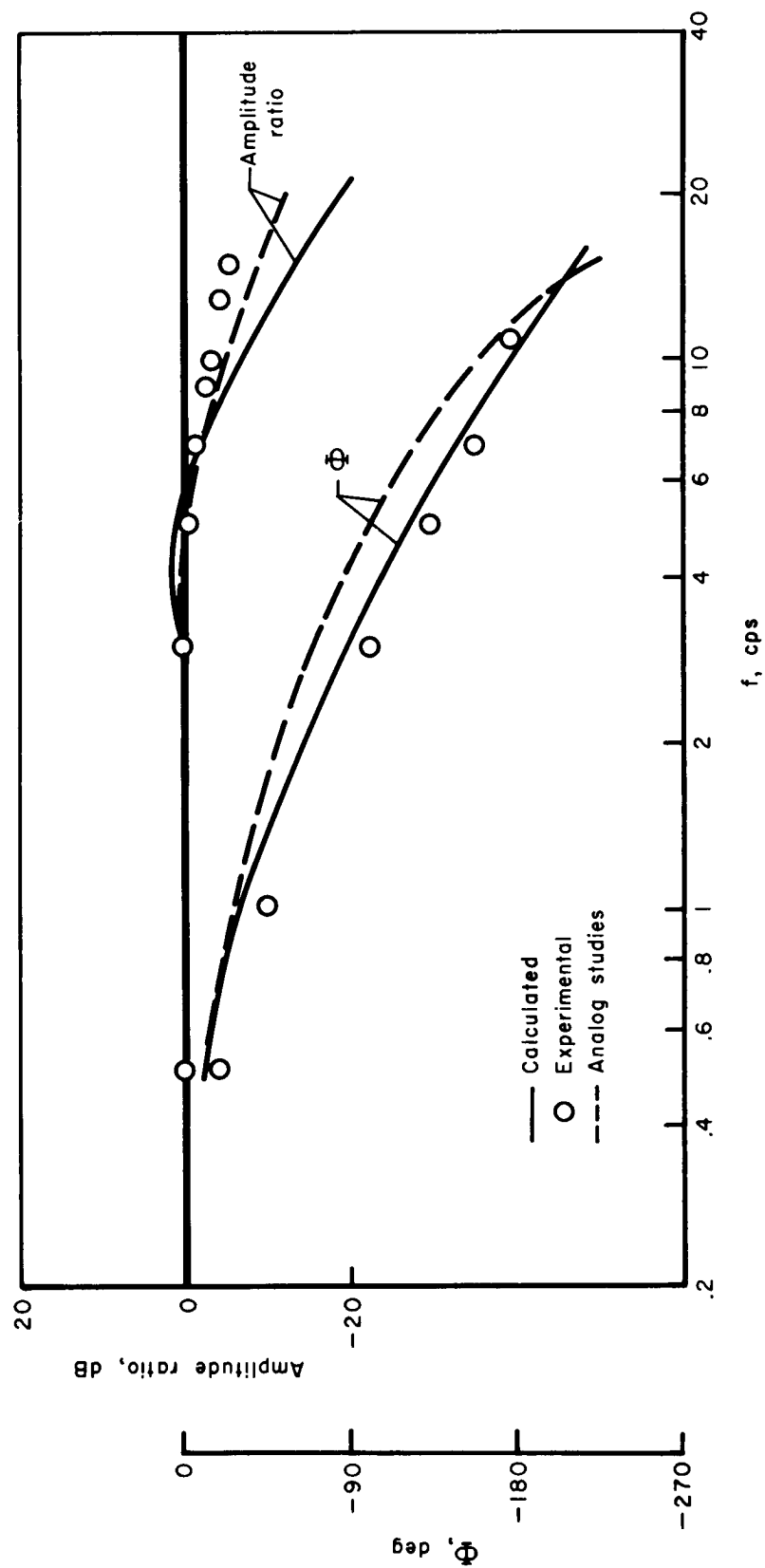


Figure 20.— Open-loop response of X-15 reaction augmentation system with production shaping.  
 Input = 10 deg/sec, dead band = 1 deg/sec.

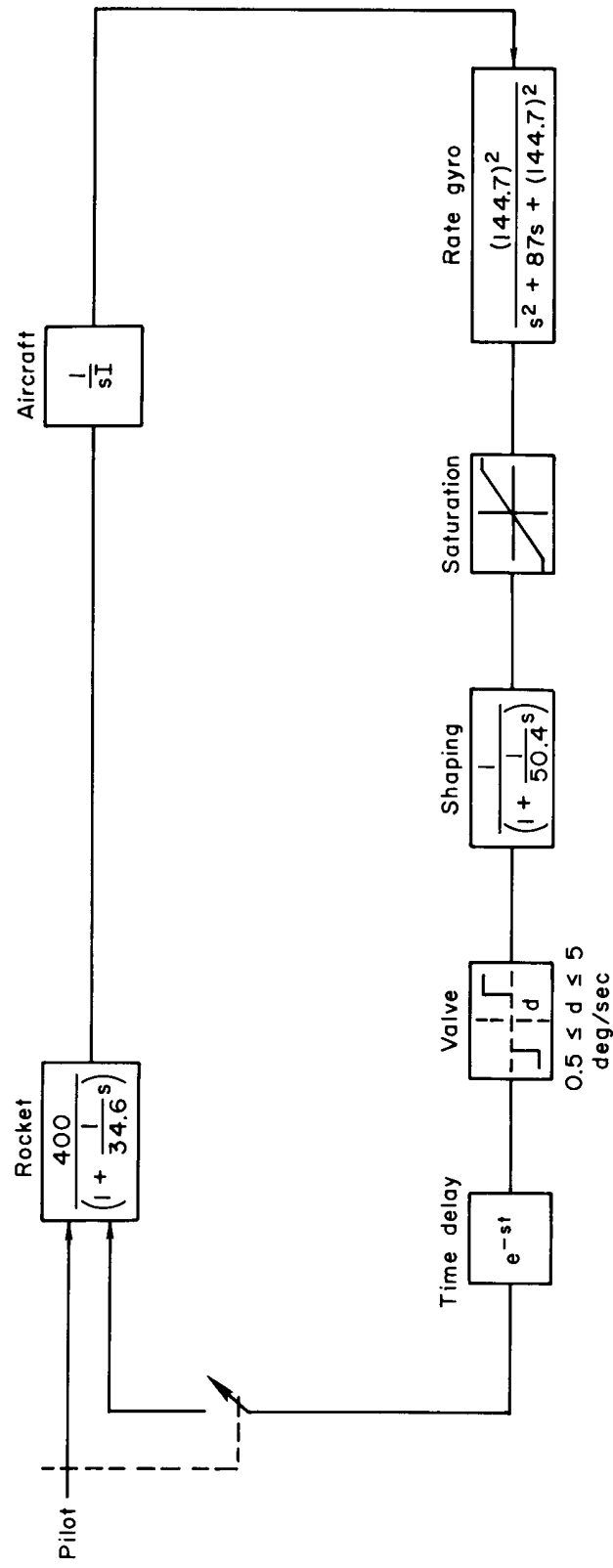


Figure 21.— Block diagram of X-15 reaction augmentation system showing component characteristics.



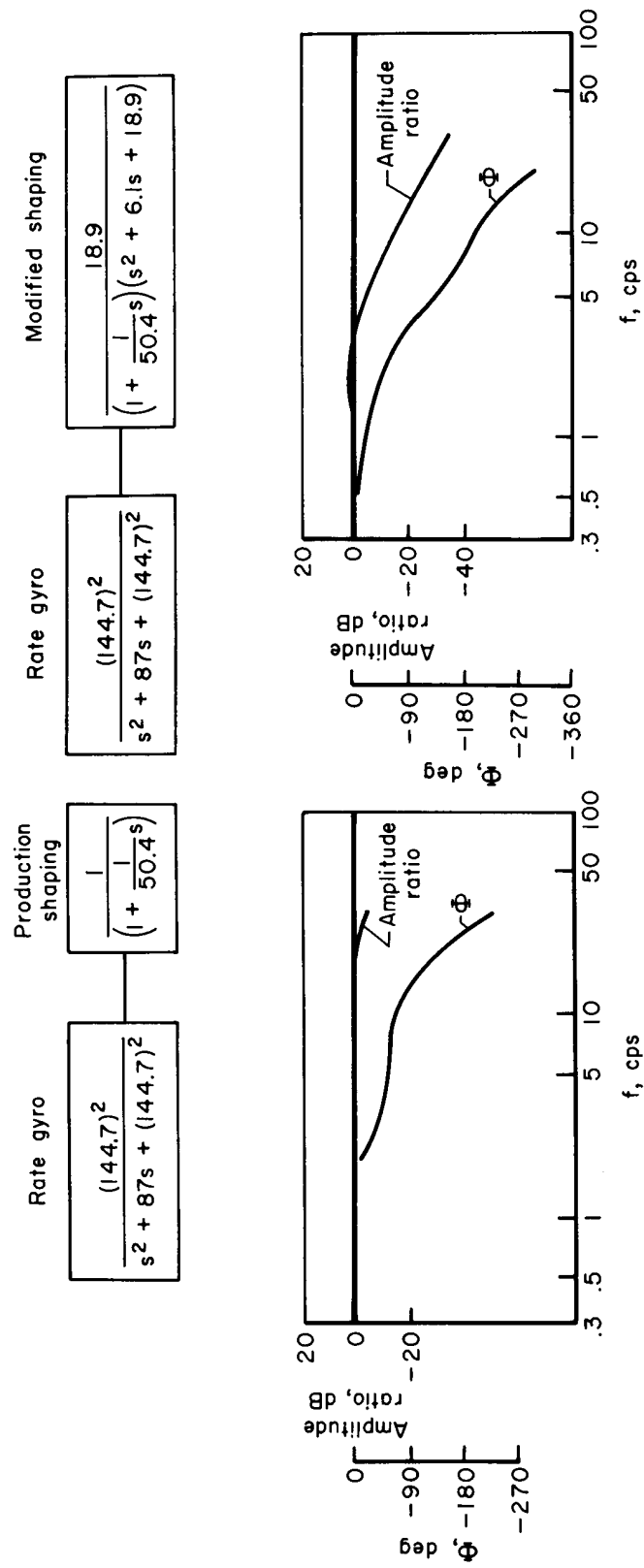


Figure 22.— Frequency-response characteristics of production and modified reaction augmentation system shapings.

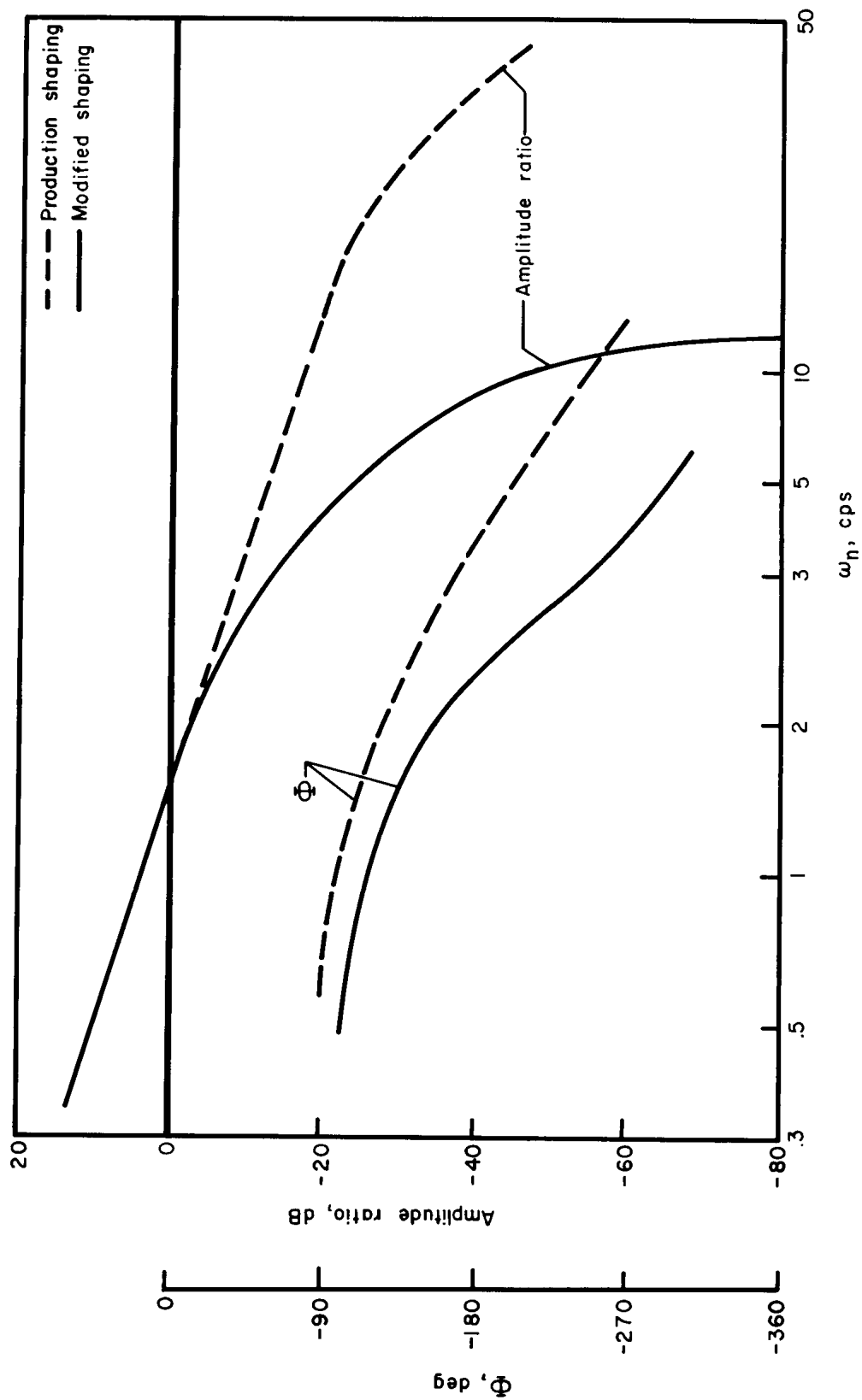


Figure 23.— Reaction augmentation system open-loop frequency-response characteristics.  
Input = 10 deg/sec, dead band = 1 deg/sec.